

X-RAY POWDER DIFFRACTION

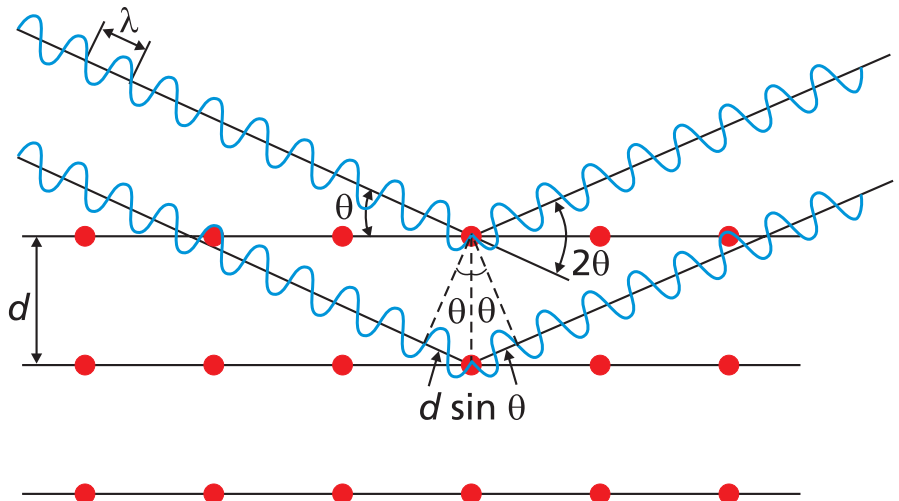
XRD for the analyst

Getting acquainted with the principles

$$n\lambda = 2d \sin \theta$$

Martin Ermrich

Detlef Opper



X-RAY POWDER DIFFRACTION

XRD for the analyst

Getting acquainted with the principles

Martin Ermrich

Detlef Opper

Published in 2011 by:

PANalytical GmbH
Nürnberg Str. 113
34123 Kassel
+49 (0) 561 5742 0
info@panalytical.de

All rights reserved. No part of this publication may be reproduced, stored in a retrieval system or transmitted in any form by any means electronic, mechanical, photocopying or otherwise without first obtaining written permission of the copyright owner.

www.panalytical.de

2nd revised edition published in 2013 by:

PANalytical B.V.
Lelyweg 1, 7602 EA Almelo
P.O. Box 13, 7600 AA Almelo, The Netherlands
Tel: +31 (0)546 534 444
Fax: +31 (0)546 534 598
info@panalytical.com

www.panalytical.com

ISBN: 978-90-809086-0-4

We encourage any feedback about the content of this booklet. Please send to the address above, referring to XRD_for_the_analyst.

Contents

1.	Introduction	7
2.	What is XRD?	8
3.	Basics of XRD	10
3.1	What are X-rays?.....	10
3.2	Interaction of X-rays with matter.....	11
3.3	Generation of X-rays.....	12
3.3.1	Introduction.....	12
3.3.2	The sealed X-ray tube.....	12
3.3.3	White radiation.....	13
3.3.4	Production of characteristic X-rays.....	14
3.4	A short introduction to crystallographic terminology.....	17
3.5	The powder diffractogram.....	21
3.5.1	Introduction.....	21
3.5.2	The position of the reflections: Bragg's law.....	22
3.5.3	The intensity of the reflections.....	25
3.5.4	The shape of the reflections.....	25
3.6	Overview of X-ray scattering techniques.....	26
3.6.1	Single crystal XRD.....	26
3.6.2	Powder diffraction.....	26
3.6.3	Special X-ray techniques.....	26
3.7	General terms used in X-ray powder diffraction.....	27
4.	The X-ray diffractometer	30
4.1	Introduction.....	30
4.2	Geometries.....	30
4.2.1	Reflection geometry.....	30
4.2.2	Transmission geometry.....	32
4.2.3	Parallel beam geometry.....	32
4.2.4	Microspot analysis.....	33
4.3	Optical components in the X-ray beam path.....	33
4.3.1	General requirements.....	33
4.3.2	Slit optics for Bragg-Brentano geometry.....	33
4.3.2.1	Divergence and anti-scatter slits.....	34
4.3.2.2	Soller slits.....	35
4.3.3	Optical modules.....	36
4.4	Detectors.....	38
4.4.1	General remarks.....	38
4.4.2	Detector types.....	40
4.4.3	Comparison of the detector types.....	42
5.	XRD data collection	44
5.1	Sample preparation.....	44

5.1.1	Ideal powder	44
5.1.2	Sample types	44
5.1.3	Reflection mode	46
5.1.4	Foil transmission	46
5.1.5	Capillaries	46
5.2	Measurements	47
5.2.1	Optimum measurement conditions	47
5.2.2	Resolution	47
5.2.3	Low quantities	48
5.2.4	Air-sensitive / hygroscopic materials	49
5.2.5	Minimization of texture	49
5.2.6	Thin layers	51
5.2.7	Rough surfaces	52
5.2.8	Standard materials	52
6.	Qualitative phase analysis	54
6.1	Data processing	54
6.2	The search/match procedure; reference databases	55
6.3	Cluster analysis	56
7.	Quantitative phase analysis	58
7.1	Basics	58
7.2	Special problems	59
7.2.1	Preferred orientation	59
7.2.2	Absorption and micro-absorption	60
7.2.3	Limit of detection, limit of quantification, amorphous amounts and crystallinity	62
7.3	Methods of quantitative phase analysis	63
7.4	Examples	66
7.4.1	Discussion of different methods	66
7.4.2	Determination of retained austenite	69
7.4.3	Quantification of cement	69
8.	Crystallographic analysis	71
8.1	Indexing	71
8.1.1	Lattice parameter determination and refinement	71
8.1.2	Structure refinement	72
8.1.3	Structure solution	72
9.	Microstructural analysis	73
9.1	Residual stress	73
9.1.1	Basics	73
9.1.2	$\sin^2 \psi$ method	74
9.2	Texture	75
9.2.1	Basics	75
9.2.2	The Lotgering factor	76
9.2.3	Omega scan	77
9.3	Crystallite size determination	77

9.3.1	Basics	77
9.3.2	Crystallite size	77
9.3.3	Micro-strain	78
9.3.4	The Williamson-Hall plot	78
9.3.5	Discussion of the peak broadening	80
10.	Non-ambient XRD	81
10.1	Temperature	81
10.1.1	Correct sample positioning and height	82
10.1.2	Sample and preparation	82
10.1.3	Temperature measurement and calibration	83
10.1.4	Special requirements	83
10.2	Pressure	86
10.3	Humidity	86
11.	Recommended literature	87
12.	Symbols	90
	Index	92


PANalytical
PANalytical
PANalytical

About the author

Dr. Martin Ermrich studied Physics at the Technical University in Dresden. In 1997 he founded his own X-ray laboratory with a special focus on X-ray diffraction.

PANalytical

PANalytical



PANalytical



PANalytical



PANalytical

1. Introduction

As a (future) user of a PANalytical X-ray diffractometer you can perform almost all types of diffraction applications, depending on the configuration of your system. To get the best possible results out of your system, this book gives you an introduction to X-ray powder diffraction (XRPD or, mostly used, XRD) and provides helpful information. It gives a simple explanation of how a diffractometer works and how XRD analysis is done. This book is intended both for people new to the field of XRD analysis and for more experienced users to find new applications which might be helpful in daily work. This book avoids complex mathematical equations and understanding its contents only requires a basic knowledge of crystallography, mathematics and physics. It is not dedicated to specific diffractometer configurations or application areas, but aims to give a global overview of the various possibilities in XRD.

Chapter 2 briefly explains XRD and its benefits. General application fields are presented. Chapter 3 gives an introduction to the physics and crystallography of XRD, while Chapter 4 describes how this is used for diffraction experiments. Chapter 5 explains the XRD data collection. This includes presentation of sample preparation and measurement procedures to get the best possible results. In Chapters 6-9 the procedures to perform qualitative and quantitative phase analysis are presented. Chapter 10 deals with non-ambient XRD and describes its methods and applications together with other techniques. Chapter 11 lists recommended literature for further information on XRD analysis.

Since this book is intended to give an introduction to standard powder diffraction techniques, it does not cover other X-ray techniques like single crystal diffraction, high-resolution XRD of heteroepitaxial layers, or small-angle X-ray scattering (SAXS).

Other books from PANalytical in this series:

- | | |
|------------------|---|
| P. Brouwer: | Theory of XRF – Getting acquainted with the principles |
| P. Kidd: | XRD of gallium nitride and related compounds: strain, composition and layer thickness |
| M. van der Haar: | XRF applications in the semiconductor and data storage industry |
| J.P. Willis: | XRF sample preparation – Glass beads by borate fusion |

2. What is XRD?

X-ray diffraction (XRD) is a versatile, non-destructive analytical method to analyze material properties like phase composition, structure, texture and many more of powder samples, solid samples or even liquid samples.

Identification of phases is achieved by comparing the X-ray diffraction pattern obtained from an unknown sample with patterns of a reference database. This process is very similar to the identification of finger prints in crime scene investigations. The most comprehensive database is maintained by the ICDD (International Centre of Diffraction Data). Alternatively, it is possible to build up a reference database from experimental diffraction patterns of pure phases and/or patterns published in the scientific literature or derived from own measurements.

Modern computer-controlled diffractometer systems like the PANalytical X'Pert Powder or Empyrean in combination with phase analysis software (e.g. HighScore) use automatic routines to measure and interpret the unique diffractograms produced by individual constituents in even highly complex mixtures.

The main topics of X-ray diffraction are:

- Qualitative and quantitative phase analysis of pure substances and mixtures
- Analysis of the influence of temperature and/or other non-ambient variables, such as humidity or applied pressure
- Analysis of the microstructure of the material, including properties like crystallite size, preferred orientation effects and residual stress in polycrystalline engineered materials.

Many of these techniques can also be used for poly-crystalline layered materials such as coatings.

Other X-ray diffraction techniques include high-resolution analysis of hetero-epitaxial layers, X-ray reflectometry on thin films and small-angle X-ray scattering. These techniques are explained here briefly. More detailed information can be found in dedicated literature.

X-ray powder diffraction is used in a wide variety of research and process control environments. For example:

- Characterization of (new) materials at universities and research centers
- Process control in several industries like building materials, chemicals, pharmaceuticals, for instance phase composition and content
- Determination of polymorphism, API (active pharmaceutical ingredient) concentration determination, API stability studies in the pharmaceutical industry
- Phase identification of minerals in geological samples
- Optimization of fabrication parameters for wear-resistant ceramics and biomaterials
- Determination of the crystallinity of a phase
- Determination of amorphous phase contents in mixtures

A typical powder pattern is given in Figure 1. It shows a scan of a mixture of a crystalline phase (quartz) and an amorphous component (glass).

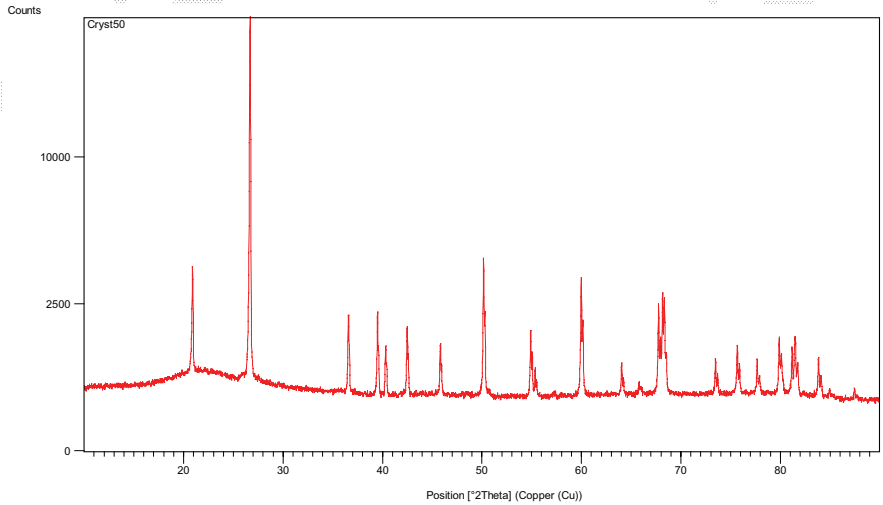


Figure 1. Typical powder pattern showing the presence of a crystalline phase and an amorphous phase

PANalytical

PANalytical

PANalytical

3. Basics of XRD

3.1 What are X-rays?

X-rays are electromagnetic waves with associated wavelengths, or beams of photons with associated energies. Both views are correct, and the view that you use at a particular time usually depends on the specific phenomena that you are interested in. Other electromagnetic waves include visible light, radio waves and γ -rays. Figure 2 shows that X-rays have wavelengths and energies between those of γ -rays and ultraviolet light. The wavelengths of X-rays are in the range from 0.01 nm to 10 nm, which corresponds to energies in the range from 0.125 to 125 keV.

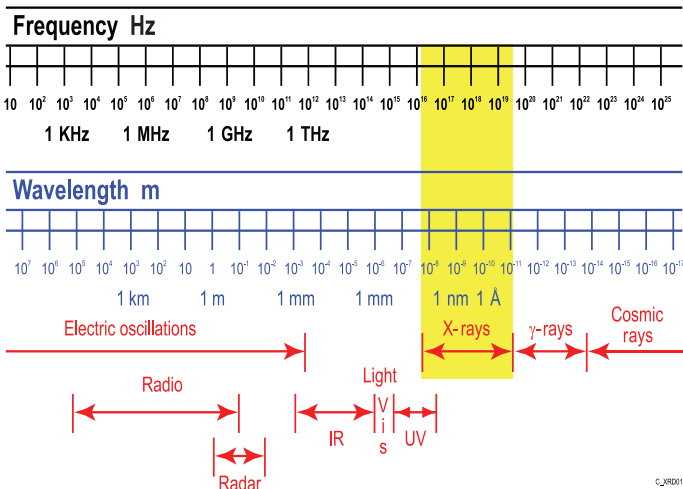


Figure 2. X-rays and other electromagnetic radiations

The wavelength λ of X-rays is inversely proportional to its energy E , according to:

$$E = h\nu = h \frac{c}{\lambda}$$

where h is the Planck's constant, ν is the frequency, and c the velocity of light.

The unit Å (Ångström), which is a unit length of 10^{-10} m, or 0.1 nm, is historically used in X-ray diffraction because it simplifies the notation of wavelengths, atomic distances and lattice parameters.

3.2 Interaction of X-rays with matter

If X-rays with a wavelength λ and an intensity I_0 penetrate a material, they become attenuated (μ), absorbed (τ), scattered (σ) and undergo the so-called 'pair-building' (π). These parameters act additively. The absorption is the first-order effect for X-rays in matter, hence the literature often does not distinguish between the attenuation and the absorption coefficient. Division by the density (ρ) yields the mass attenuation coefficient (μ/ρ), also referred to in the literature as MAC. The transmitted intensity I depends on the incident intensity I_0 , the attenuation coefficient μ and the path length through the material d :

$$I = I_0 e^{-\mu d}$$

The attenuation coefficient (μ) of the material depends on

- atomic number (Z)
- density (ρ)
- packing fraction (p) (a typical value is between 0.6 to 0.8)
- wavelength (λ)

with the following relationship: $\mu \sim \rho p Z^3 \lambda^3$

The attenuation increases steadily with the wavelength, interrupted by sharp discontinuities. These discontinuities correspond to the absorption edges caused by electronic shells of the atoms, see Chapter 3.3.4.

With respect to the scattering process, two main interactions of X-rays with matter have to be distinguished: coherent and incoherent scattering.

- **Coherent** or Rayleigh scatter is the most important effect for X-ray diffraction: it is the elastic scattering of the incoming photon upon collision with inner-shell electrons. The wavelength of the photon is not changed, i.e. the photon energy remains constant.
- **Incoherent** scatter can be divided into Compton scatter and fluorescence. In both cases, the wavelength of the photon increases by the scattering process, i.e. the photon energy decreases.
 - **Compton scatter**: an electron is pushed out of its shell or is excited to a higher energy state. The incoming X-ray photon loses energy. This type of scatter can be ignored in laboratory X-ray powder diffraction because of the low energy of the incoming photons.
 - **Fluorescence**: the incoming photon ejects an inner-shell electron from the atom. The vacancy is then filled by an electron from one of the atom's outer shells. The action of this electron moving from one shell to another creates an X-ray photon with the energy difference of the two shells. The energy of this photon is dependent on the atomic number and is therefore characteristic for the atom itself. This effect is used in XRF (X-ray fluorescence) analysis for determination of elemental concentrations. In XRD it is generally considered as an unwanted radiation because it raises the background of the diffractogram and reduces the peak/background ratio.

3.3 Generation of X-rays

3.3.1 Introduction

There are several physical methods of obtaining X-rays of sufficient intensity for X-ray diffraction. The most common methods are:

- Bombarding a target of a suitable material (anode) with a focused electron beam. The maximum achievable X-ray intensity is limited by the maximum power, which is restricted by the cooling system of the stationary anode. These X-ray sources are called *sealed X-ray tube*. Modern designs use ceramic insulators instead of glass bodies to improve stability and lifetime. These tubes are widely used in modern laboratory diffraction systems, like the X'Pert PRO and Empyrean.
- Deflection of high-energy electrons by electromagnetic fields, yielding emission of X-rays. This principle is used in synchrotrons. These instruments yield a very strong X-ray intensity but are large and costly to operate so that they are available only in huge research centers, mainly used by scientists.

3.3.2 The sealed X-ray tube

In a sealed X-ray tube (see Figure 3), electrons are emitted by a hot filament, the cathode. The high voltage difference (U) between cathode and anode accelerates the electrons with a high speed towards the anode material, resulting in a line image of the filament on the anode. The kinetic energy ($E_{\text{kin}} = e \cdot U$) of the electrons is converted mainly into heat (99%) and X-ray radiation (1%). Hence the (back side of the) anode has to be cooled effectively.

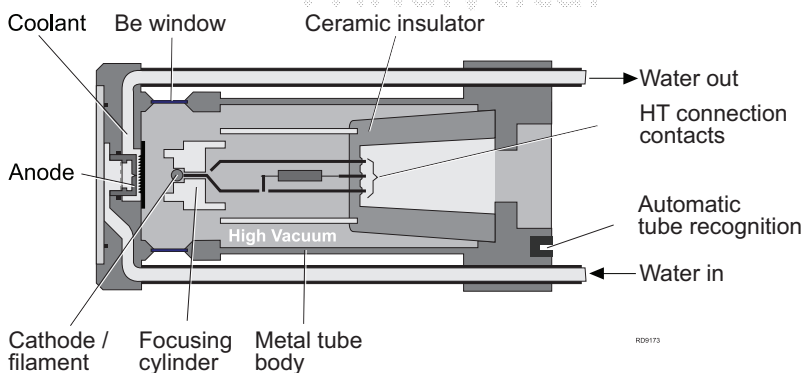


Figure 3. Schematic drawing of ceramic X-ray tube (X'Pert type)

X-rays are emitted from the tube anode through thin beryllium windows. The windows keep the tube sealed and allow X-rays to pass through. Optics are 'looking' to the anode under a grazing angle, which results in a smaller apparent source spot size. The windows are located at parallel or perpendicular positions with respect to the focal line to form the point or line focus. In a typical long fine

focus tube the line focus has a dimension of 0.04 mm × 12 mm, point focus of 1.2 mm × 0.4 mm. Both focal positions have their typical applications, which are:

- Line focus:
 - High-resolution phase analysis
 - Omega stress
- Point focus:
 - Micro-diffraction
 - Texture
 - Psi stress

These applications are explained in more detail in subsequent chapters.

The intensity of the X-ray tube decreases with time. This is mainly caused by the evaporation of the tungsten filament (the cathode) leading to deposition of tungsten on the anode and the Be windows. A deposition of tungsten on the anode leads to additional lines in the diffractogram.

When the electrons hit the anode, two types of radiations are emitted: *white radiation* (bremsstrahlung) and the *characteristic X-ray radiation*.

3.3.3 White radiation

The interaction of the accelerated electrons with the anode leads to a loss in energy, resulting in the emission of X-rays in a continuous spectrum, the so-called *white radiation* or *bremsstrahlung*.

The **Duane-Hunt law** gives an estimation of the lowest wavelength λ_0 of the radiation wavelength, starting with the energy balance:

$$E = eU = hv = h \frac{c}{\lambda}$$

- e elementary charge
- U used high voltage of the tube
- c velocity of light
- h Planck constant
- v frequency

$$\text{It therefore follows: } \lambda_0 = \frac{hc}{eU} \Rightarrow \lambda_0 (\text{\AA}) = \frac{12.4}{U(\text{kV})}$$

The **Dauvillier law** allows the estimation of the wavelength λ_{\max} of the maximum of the radiation wavelength:

$$\lambda_{\max} = (\text{between } 1.5 \text{ and } 1.7) \lambda_0$$

The total intensity I_{wr} of the white radiation wavelength is:

$$I_{\text{wr}} \sim ZU^2i$$

With Z atomic number
 U tube voltage
 i used emission current of the tube

It can be derived that:

- the X-ray intensity is linearly dependent on the emission current i
- it is quadratically dependent on the acceleration voltage U
- targets with higher atomic number deliver a higher X-ray intensity, this is caused by the larger atomic radius (a more effective cross section)

White radiation is unwanted for most X-ray diffraction experiments, the majority of diffraction experiments require a monochromatic radiation.

3.3.4 Production of characteristic X-rays

In order to understand the principles of the production of characteristic radiation we will refer to the Bohr 'shell' model.

An atom consists of a nucleus with positively charged protons and neutrons without any charge. The nucleus is surrounded by electrons grouped in shells or orbitals. The innermost shell is called the *K*-shell, moving outwards followed by *L*-shells, *M*-shells and so on. The *L*-shell has 3 sub-shells called L_{I} , L_{II} and L_{III} . The *M*-shell has 5 sub-shells M_{I} , M_{II} , M_{III} , M_{IV} and M_{V} . The *K*-shell can contain 2 electrons, the *L*-shell 8 and the *M*-shell 18. The energy of a specific electron depends on the shell and on the proton number (i.e. the chemical element). Irradiating an atom with X-ray photons or electrons with sufficient energy can expel an electron from the atom (Figure 4).

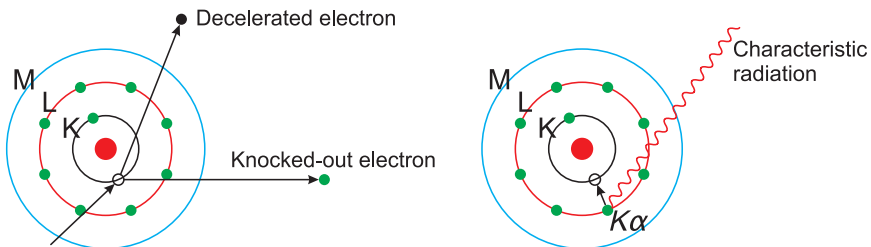


Figure 4. Production of characteristic radiation

The emission of an electron produces a void in a shell (in the example a void in the *K*-shell). This puts the atom in an excited state with a higher energy. The atom wants to restore the original configuration by releasing the excess energy. This is

done by transferring an electron from an outer shell - in this case from the L -shell - to the void in the K -shell. An L -shell electron has a higher energy than a K -shell electron. Thus when an L -shell electron is transferred to the K -shell, the energy excess is emitted as an X-ray photon. The emission energy of the photon is seen as a certain line in the spectrum. The energy of the emitted X-ray photon depends on the difference in energy of the shell with the initial void and the energy of the electron that fills the void (in the example, the difference between the energy of the K - and the L -shell). Each atom has its specific energy levels, so the emitted radiation is characteristic for that atom (in this case that of the anode material).

To expel an electron from an atom, the X-rays must have a higher energy than the binding energy of the electron. If an electron is expelled, the incoming X-ray photon is absorbed, leading to scattering. If on the other hand the energy is too high, many photons will 'pass through' the atom and interaction with atoms will only occur occasionally. Figure 5 shows that high energies are hardly absorbed. If the energy is reduced the absorption increases and the scattering yield goes up. The highest yield is reached when the energy of the photon is just above the binding energy of the electron to be expelled. If the energy becomes lower than the binding energy, a jump or edge can be seen: the energy is too low to expel electrons from that shell, but is too high to expel electrons from the lower energetic shells. The figures show the K -edge corresponding to the K -shell, and three L -edges corresponding with the L_I -, L_{II} - and L_{III} -shells.

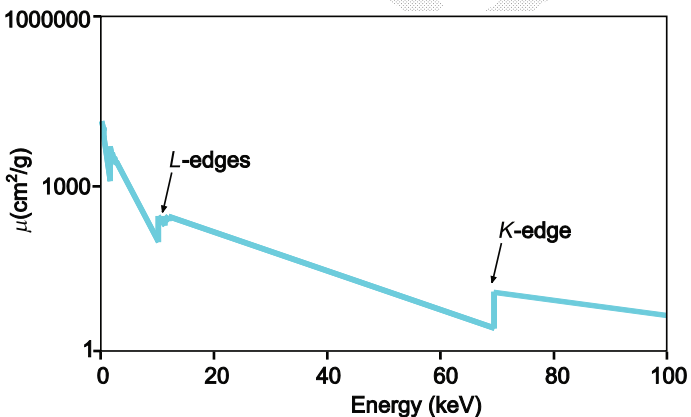


Figure 5. Mass absorption coefficient vs. photon energy

Based on quantum mechanics not all transitions are allowed. For instance a transition from the L_I to the K -shell. Figure 6 gives an overview of the most important emission lines with their transitions.

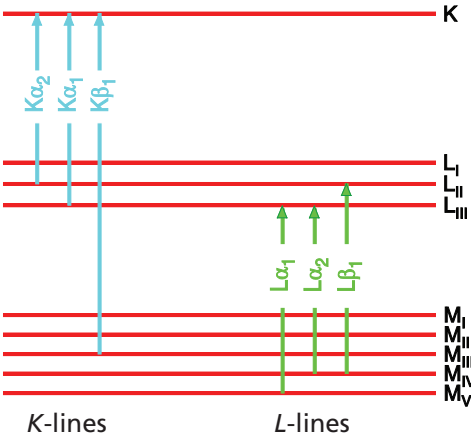


Figure 6. Major lines and their transitions

Because each atom has its own energy levels, the emitted radiation is specific to that atom: the so-called *characteristic X-ray radiation*. This procedure is the basis of X-ray fluorescence analysis (XRF). The wavelength of the photon depends on the atomic number Z following the **Moseley law**:

$$\frac{1}{\lambda} \sim Z^2$$

An X-ray tube delivers the characteristic wavelengths of its anode material (most commonly Cu, Co, or Mo). The characteristic radiation is superimposed on the white radiation.

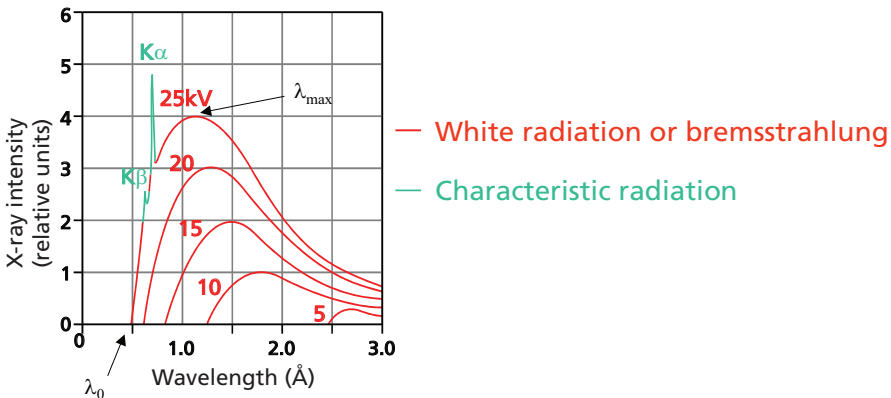


Figure 7. The total X-ray spectrum for various acceleration voltages (Mo X-ray tube)

Figure 7 shows the X-ray spectrum for various acceleration voltages, in this case for a Mo X-ray tube. One can see that if the voltage is too low, the amount of characteristic radiation is very small. If the excitation voltage is too high, the amount of white radiation increases over the amount of characteristic radiation. This leads to a high background in the diffractogram. The photon yields are described in Chapter 3.3.3.

Each anode material has its own optimal voltage for the production of characteristic X-rays. This is approximately four times the energy of the $K\alpha$ line of the anode material (Table 1).

Table 1. Optimal excitation voltages for different anode materials

Anode material	Mo	Cu	Co	Cr
$K\alpha$ energy (keV)	17.4	8.0	6.9	5.4
U_{opt} (kV)	60-50	40	30	25-20

As already mentioned, the characteristic spectrum has several lines: the ' $K\alpha$ doublet', consisting of $K\alpha_1$ and $K\alpha_2$ radiation, as well as $K\beta$ radiation. In order to achieve monochromatic $K\alpha$ radiation, the $K\beta$ line is generally suppressed by a suitable monochromator (Chapter 4.3.3) or filter.

Table 2 shows some relevant wavelengths and the corresponding attenuation filters for $K\beta$ radiation.

Table 2. Wavelengths used for XRD and attenuation filters for $K\beta$ radiation (source: ICDD, International Centre of Diffraction Data)

Anode	Wavelength (Å)			$K\beta$ -filter
	$K\alpha_1$	$K\alpha_2$	$K\beta$	
Cr	2.28970	2.29361	2.08487	V
Fe	1.93604	1.93998	1.75661	Mn
Co	1.78897	1.79285	1.62079	Fe
Cu	1.54056	1.54439	1.39222	Ni
Mo	0.70930	0.71359	0.63229	Zr

Intensity relations: $(K\alpha_1) : (K\alpha_2) : (K\beta) \approx 100 : 50 : 25$

3.4 A short introduction to crystallographic terminology

Crystal structure

A crystal structure is a unique three-dimensional arrangement of atoms in solid matter. The crystal structure is composed of a unit cell which is periodically repeated in three dimensions on a lattice. The spacing between unit cells in various directions is called its lattice parameters. The symmetry properties of the crystal are embodied in its space group. An example is given in Figure 8.

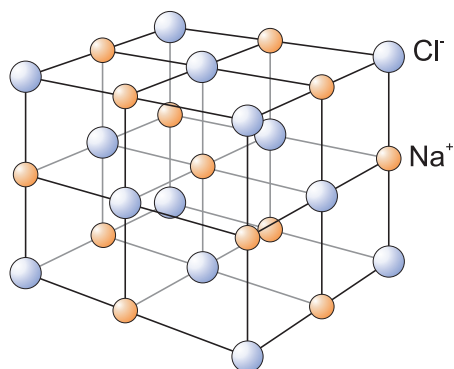


Figure 8. Crystal structure of NaCl

Unit cell

The unit cell is a spatial arrangement of atoms which is tiled in three-dimensional space to describe the crystal. The unit cell is given by its lattice parameters. These are the lengths of the cell edges and the angles between them. The positions of the atoms inside the unit cell are described by the set of atomic positions (x_i, y_i, z_i) measured from a selected lattice point.

For each crystal structure there is a conventional unit cell, which is the smallest unit that has the full symmetry of the crystal. However, the conventional unit cell is not always the smallest possible choice. A primitive unit cell of a particular crystal structure is the smallest possible unit cell one can construct such that, when tiled, it completely fills space. This primitive unit cell does not, however, display all the symmetries inherent in the crystal.

Crystalline state

The atoms are periodically and regularly arranged in three dimensions. Ideal crystals are described completely by only one unit cell and its infinite three-dimensional-periodic repetition (translation symmetry), delivering a long-range order. Crystalline material leads to pronounced peaks in powder diffractometry.

Amorphous state

In contrast to the crystalline state, in the amorphous state the structure has only a short-range order of the atoms (or unit cells). This leads to very broad humps in the diffraction pattern instead of clear diffraction peaks.

Reciprocal lattice

The reciprocal lattice is a mathematical construction that helps to deliver a description of X-ray diffraction.

Each point (hkl) in the reciprocal lattice corresponds to a set of lattice planes (hkl) in the real space lattice. The direction of the reciprocal lattice vector corresponds to the normal to the real space planes, and the magnitude of the reciprocal lattice vector is equal to the reciprocal of the interplanar spacing of the real space planes.

Bravais lattices

The Bravais lattices (see Table 3) are the 14 possible lattices given by translation symmetry. These simple lattices allow to describe all crystal structures, even complicated ones (Figure 9).

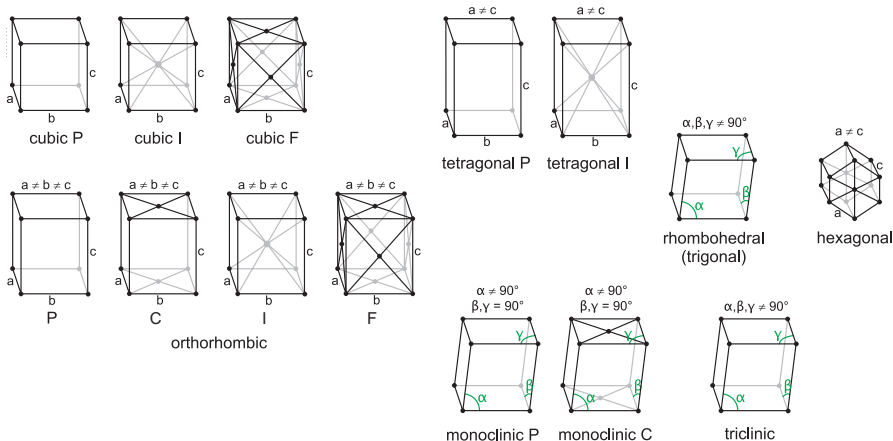


Figure 9. Graphical representation of the 14 Bravais lattices

Table 3. The 14 Bravais lattices

System	Unit cell	lattice parameters	angles
triclinic	P	$a \neq b \neq c$	$a \neq b \neq \gamma$
monoclinic	P, C	$a \neq b \neq c$	$a = b = 90^\circ \neq \gamma$
orthorhombic	P, C, I, F	$a \neq b \neq c$	$a = b = \gamma = 90^\circ$
trigonal	R	$a = b = c$	$a = b = \gamma \neq 90^\circ$
hexagonal	P	$a = b \neq c$	$a = b = 90^\circ, \gamma = 120^\circ$
tetragonal	P, I	$a = b \neq c$	$a = b = \gamma = 90^\circ$
cubic	P, I, F	$a = b = c$	$a = b = \gamma = 90^\circ$
P	primitive unit cell		
C	face-centered unit cell		
I	body-centered unit cell		
F	all-face-centered unit cell		
Some abbreviations to describe the unit cell:			
pc	primitive cubic		
bcc	body-centered cubic		
fcc	face-centered cubic		
hcp	hexagonal closed packed		

Crystal classes

A further classification of the contents of a unit cell can be made by classifying possible crystal structures into those that obey different symmetry operations: rotation, glide reflection, inversion and combinations of them. There are 32 crystal classes (also known as point symmetry groups).

Space groups

If all possible Bravais lattices and crystal classes are taken into consideration, one ends up with 230 unique space groups. Every crystal has a structure which can be described by one of the 230 space groups.

Interplanar spacings or lattice planes

It is possible to define imaginary planes in the crystal. These planes are described by the Miller indices. Their distance is $d(hkl)$.

Miller indices

The Miller indices are the designation of interplanar spacings, which cut the axes lengths a , b , c or the axis intercepts in the reciprocal space a/h , b/k and c/l , respectively. Numbers are reciprocals of the intercepts (see Figure 10). For the (102) plane for example, you have to go one step in 'a' direction and half a step in 'c'.

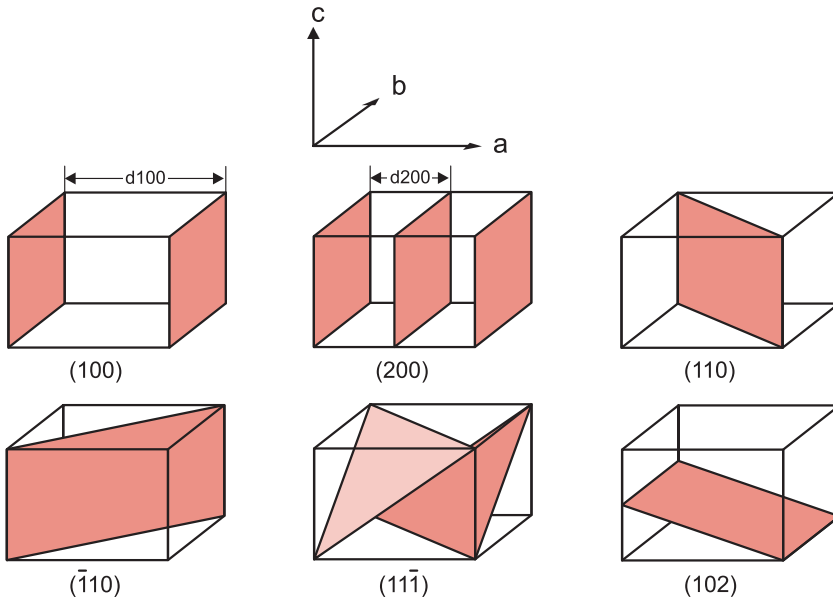


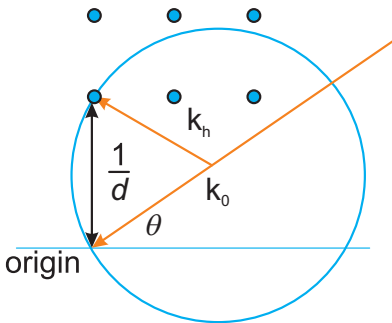
Figure 10. Examples of different lattice planes

Ewald sphere

The Ewald sphere contains all of the components that are needed to visualize the diffraction process geometrically. It is a geometric construction which demonstrates the relationship between

- the wavelength of the incident beams of light,
- the angle of diffraction for a given reflection,
- the unit cell and reciprocal unit cell of the crystal, and
- the distance between the crystal and the receiving slit/detector.

A reflection hkl fulfills the Bragg equation, if the lattice point coincides with the Ewald sphere. The radius of the Ewald sphere is $1/\lambda$ (Figure 11).



k_0 vector of the incoming beam
 k_h scattered beam in h direction

Figure 11. Graphical representation of the Ewald sphere; $r=1/\lambda$

3.5 The powder diffractogram

3.5.1 Introduction

A powder diffractogram displays the scattered intensity versus the Bragg angle (2θ). It contains a number of peaks (reflections). The peaks are characterized by their position, intensity and profile. The peaks and the background are the source of all information of the X-ray powder diffraction technique. Table 4 shows an overview.

Table 4. General survey of the information content of a powder diffractogram

Reflection	depends on	main information
Position	<ul style="list-style-type: none"> - periodic arrangement of the atoms/molecules - wavelength used 	<ul style="list-style-type: none"> - qualitative phase analysis - lattice parameters - residual stress
Intensity	<ul style="list-style-type: none"> - crystal structure - wavelength used - sample preparation 	<ul style="list-style-type: none"> - quantitative phase analysis - crystal structure - preferred orientations/texture
Profile	<ul style="list-style-type: none"> - lattice distortions 	<ul style="list-style-type: none"> - micro-strain - crystallite sizes

The origins of these three fundamental parameters are discussed in more detail in the following paragraphs.

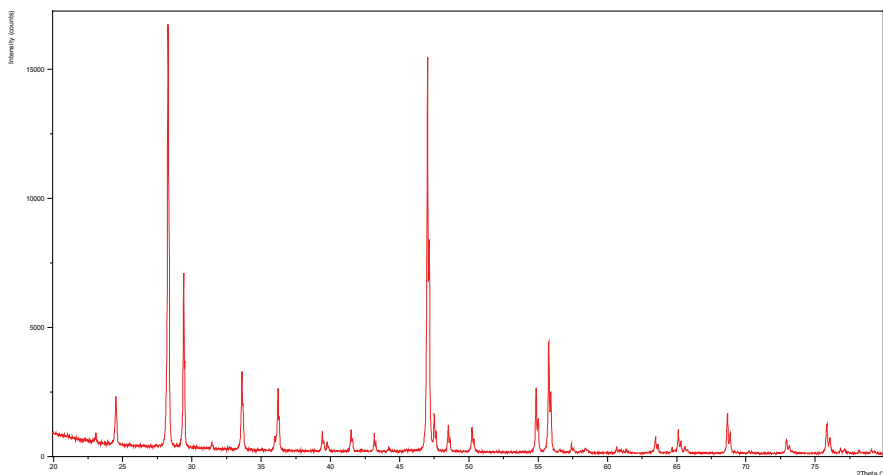


Figure 12. Typical diffraction pattern of a mineral mixture

3.5.2 The position of the reflections: Bragg's law

As a consequence of the regular arrangement of the atoms in solid matter coherent scattering of X-rays at the atoms results in constructive interference at certain well-defined angles. This effect is similar to the well-known diffraction of visible light at gratings with a nm-scaled spacing close to the light's wavelength (Figure 13). A crystal can be seen as a three-dimensional grating with a spacing of a few Ångströms, and diffraction effects can be observed when the wavelength of the incoming X-ray photon is of similar size.

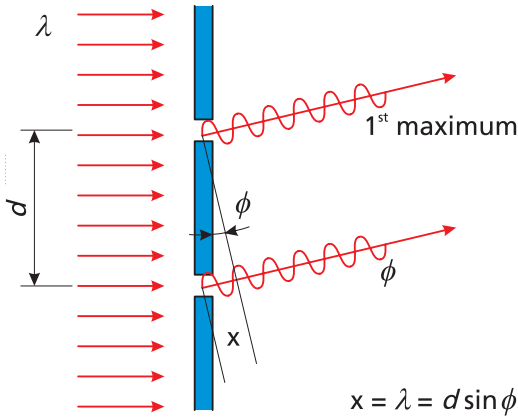


Figure 13. Constructive interference at a grating (visible light)

In 1913 W.H. Bragg and W.L. Bragg described diffraction and interference of X-rays in a crystal as reflections at the atomic planes of the crystal lattice. The positions of the reflections are calculated using the optical path difference $2s$, with $s = d \sin \theta$, between two reflected rays at neighboring interplanar spacings. As in visible light optics, maxima are produced for integer multiples of λ .

It follows: $2d \sin \theta = n\lambda$ (Bragg's law)

- d interplanar spacing d_{hkl} (hkl: Miller indices)
- θ Bragg angle θ_b
- 2θ : angle between incident and reflected beam
- n 'order' of the interference $n = 1, 2, 3 \dots$, normally $n = 1$
(called : reflection of order n)
- λ wavelength

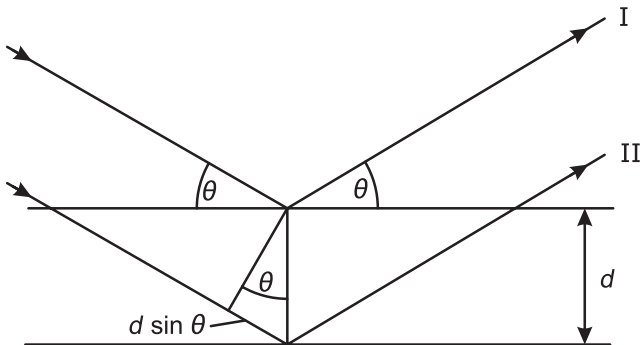


Figure 14. Graphical representation of Bragg's law

Discussion of Bragg's law

1. The interplanar spacing (d) between the different lattice planes is characterized by the Miller indices hkl (d_{hkl}). So, d_{100} means the spacing between the (100) planes.
2. The order n of interferences is described by higher (hkl), i.e. the second order of the (111) reflection gets the indices (222). Therefore $n = 1$ is valid.
3. Bragg's law is the necessary condition for a reflection, however, certain reflections may not appear in the diffractogram as a result of destructive interference, see Chapter 3.5.3.
4. Resolution can be defined as the lowest measurable d -value for a used wavelength, for $\sin \theta = 1$ follows $d_{\min} = \lambda/2$.
5. Varying of λ causes:
 - the number of measurable reflections to vary, and
 - the angular position of the reflections to vary; also,
 - the separation between two neighboring reflections is changed.

Application: If you use Mo instead of Cu radiation, the reflections move to smaller angles and get closer together. More reflections can be measured, but coupled with decreasing resolution.

6. Knowing the d -values, it is possible to determine the lattice parameters (a , b , c , α , β , γ) using the so-called 'quadratic forms', which will be more complicated with lower symmetry. Simple examples:

cubic system
$$\frac{1}{d^2} = \frac{h^2 + k^2 + l^2}{a^2}$$

tetragonal system
$$\frac{1}{d^2} = \frac{h^2 + k^2}{a^2} + \frac{l^2}{c^2}$$

7. Sometimes it is confusing that different terms are used having the same meaning:
 - *Diffraction* in the sense of the interaction of waves at a lattice, yielding interferences.
 - *Reflection* in the sense of a reflection at the interplanar spacings.

3.5.3 The intensity of the reflections

The intensity of a reflection is mainly determined by the following parameters:

- the structure factor, which is determined by
 - the symmetry of the crystal,
 - the positions of the atoms in the unit cell,
 - the number of electrons of the atoms (the amplitude of the diffracted wave is quadratically dependent on this number).
- the amount of material
- the absorption in the material

All factors that determine the absolute intensity are discussed in Chapter 7.1.

Example: the CsCl (100) reflection

For this particular d -spacing, the wave front constituted of waves originating from both atom types show an interference that is partly destructive because both waves are in anti-phase with respect to each other (see wave front A-B, Figure 15), in other words: the d_{100} reflection will be weak. Depending on the material and specific reflections, also amplification or even complete extinction of a particular reflection can occur.

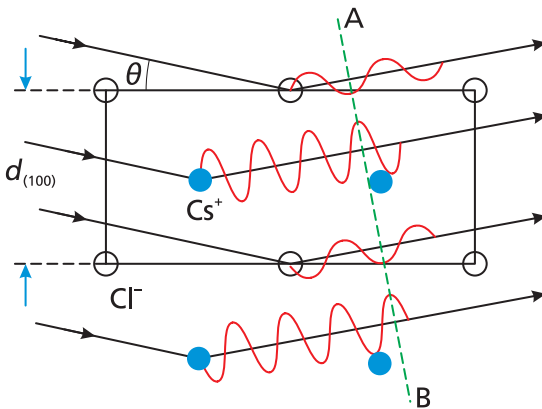


Figure 15. Wave fronts in CsCl for d_{100}

Systematic extinction is quite common in materials with a high symmetry, for instance in body-centered cubic (bcc) materials (for example α -Fe or W) only those reflections obeying the rule $h + k + l = 2n$ (n is an integer number) are visible. In other words: the (100) and (111) reflections are not observed, the diffractogram starts with the (110) reflection.

3.5.4 The shape of the reflections

The factors that influence the width and the overall shape of the reflections can be divided into two main categories:

- Instrument-related effects: determined by the diffractometer geometry, the particular X-ray optical components and their settings, as well as the detection system. This is discussed extensively in Chapter 5.
- Sample-related effects: mainly the average crystallite size and the micro-strain resulting from defects in the crystal lattice. This is further described in Chapter 9.3.

3.6 Overview of X-ray scattering techniques

3.6.1 Single crystal XRD

In single crystal X-ray diffraction, a single crystal is rotated around various axes in order to find a large number of different reflections. The atomic arrangement within the crystal (the crystal structure) can be determined from the angular positions and the intensity of these reflections.

A four-circle goniometer is required in order to observe all possible reflections. Single-crystal diffractometers are dedicated instruments, mainly used in research institutes and departments.

3.6.2 Powder diffraction

In X-ray powder diffraction, the sample consists of an infinitely large number of small crystallites, ideally randomly oriented with respect to each other. Because all orientations are present, it is only necessary to vary the angle of incidence and the angle of diffraction. A powder diffractogram is obtained by counting the detected intensity as a function of the angle between the incident and the diffracted beam.

3.6.3 Special X-ray techniques

SAXS (small-angle X-ray scattering)

SAXS is an analytical method of determining the structure of particle systems in terms of average sizes or shapes. The materials can be solid or liquid and they can contain solid, liquid or gaseous domains (so-called particles) of the same or another material in any combination.

Because the SAXS technique looks at particle distances instead of atomic distances, the effects appear at very small scattering angles near the primary beam. Many of these measurements can be done on a standard powder system like X'Pert Powder or Empyrean. The experiments are carried out in transmission geometry, using X-ray mirrors and a dedicated collimation slit system. There are special cases which require a dedicated SAXS instrument.

PDF (pair distribution function) analysis

Pair distribution function analysis is a technique to investigate all kinds of material, like amorphous and nanocrystalline materials, or even liquids. This technique determines average distances between neighboring atoms.

One can calculate or refine a structure model by mathematical treatment of the scattering data. PDF analysis can be done with a standard laboratory diffractometer by using short wavelengths like Mo or (better) Ag radiation. Short wavelengths lead to a large set of recorded d -values and provide more information for subsequent mathematical modelling.

High-resolution XRD

High-resolution X-ray diffraction (HR XRD) is widely used to investigate the match of heteroepitaxial layers to a single crystal substrate. These layers have very small differences in their d -spacing compared with the substrate. Thus the reflections of substrate and layer have a very close distance in 2θ . This requires a highly monochromatic X-ray beam with very low divergence in combination with a high-resolution goniometer.

The technique is commonly used in the research and production of compound semiconductor materials and is described extensively in the book 'X-ray Scattering from Semiconductors' by Paul F. Fewster (ISBN 1-86094-360-8).

X-ray reflectometry (XRR)

When X-rays penetrate the interface between two materials with a different density (ρ) the X-rays can be refracted or even reflected, depending on the density difference, the wavelength of the incoming beam and the angle of incidence. Layer systems on a substrate produce both constructive and destructive interference. The measurement of the reflection intensity versus 2θ leads to a reflectivity curve. The shape of this curve allows characterization of:

- layer thickness
- layer density
- surface / interface roughness
- quality of layers / interfaces

3.7 General terms used in X-ray powder diffraction

Diffractogram (or diffraction pattern)

A diffractogram is a representation of intensity vs. diffraction angle, which is in contrast to other 'spectra', representing intensity versus energy or wavelength.

Resolution

In powder diffraction, resolution is defined as the ability to separate two (or more) neighboring reflections. In single crystal diffraction it is defined as the *lowest* possible d -value, which can be measured with an instrument. In small-angle X-ray scattering it is the *highest* possible d -value.

Particle size and crystallite size

XRD line profile analysis is used to determine the crystallite sizes. The crystallite size corresponds to the size of the coherent scattering domain. Therefore estimations of the average crystallite size from X-ray diffraction generally lead to smaller values than particle size determinations.

Particle sizes are normally determined using special particle size analyzers or electron microscopy methods, but SAXS also provides information about particle sizes, typically in the 1-100 nm range.

Crystallinity

Crystallinity describes the percentage of the crystalline part in a mixture of crystalline and amorphous materials (known as the crystallinity index or % crystallinity). Note that crystallinity is often synonymously used to describe the quality of the crystal itself in terms of lattice defects, micro-strain etc.

Measurements at low angles

'Low-angle diffraction' or 'small-angle diffraction' are terms used for several, very different, techniques:

1. The classical small-angle X-ray scattering (SAXS) as described in Chapter 3.6.3
 - measurements are done very close to the primary beam
 - is used for size determination of particles or pores
2. The so-called 'thin film' measurements
 - performed in parallel beam geometry on a standard goniometer. The incident angle is very small compared to the diffracted beam angle. It is used for phase analysis of the sample surface or surface layers. Variation of the incident angle allows the analysis of graded layers or multi-layer systems.
3. Qualitative phase analysis
 - measurements at low angles for the phase analysis of substances with large lattice parameters (for example: organic materials)
4. Reflectometry as described in Chapter 3.6.3
 - investigation of layers using the total reflection of the X-rays at layer interfaces (for example: multi-layers, NiC, WC, TaSi, Ta (see Figure 16))
 - interferences are caused by density differences at the interfaces of the layers.

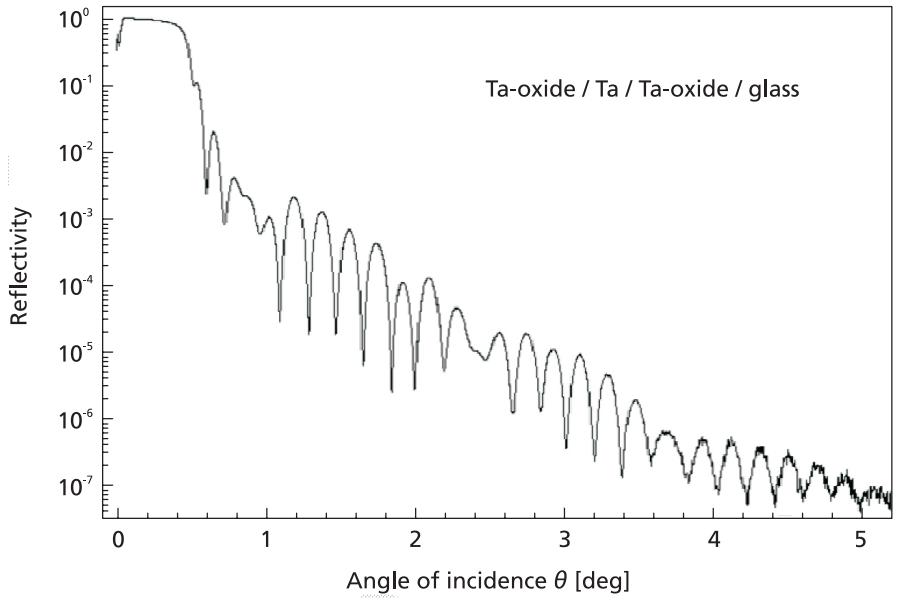


Figure 16. Example of a reflectivity curve of a multi-layer sample

PANalytical



PANalytical



PANalytical

4. The X-ray diffractometer

4.1 Introduction

In a powder diffractometer, the X-rays produced by the tube pass through primary optical components, irradiate the sample, are diffracted by the sample phases, pass secondary optical components and enter the detector. By varying the diffraction angle (2θ , the angle between the incident and the diffracted beam) through movements of tube or sample and detector, intensities are recorded to create a diffractogram.

Depending on the diffractometer geometry and the type of sample, the angle between the incident beam and the sample is either fixed or variable, normally coupled to the diffracted beam angle.

4.2 Geometries

There are two main methods to investigate a powder sample with X-rays:

- Reflection geometry: the X-rays are scattered by a flat sample surface,
- Transmission geometry: the X-rays pass through an X-ray transparent sample, which can be prepared as:
 - a sample between foils,
 - a thin solid sample, transparent for X-rays,
 - a sample in a glass capillary.

The preferable method depends on the sample type as discussed in the following sections.

4.2.1 Reflection geometry

Figure 17 shows a typical diffractometer setup in the Bragg-Brentano, or reflection geometry. This geometry is the most commonly used geometry for phase analysis. The focal spot of the tube, the sample surface and the detector slit are positioned on the so-called focusing circle.

In addition the focal spot of the tube and the detector slit are positioned on the so-called measuring circle (here the sample surface is the circle center). But, because the sample is normally flat, the beam path is para-focussing. In a real focusing geometry, the sample should be slightly curved to exactly match the focusing circle.

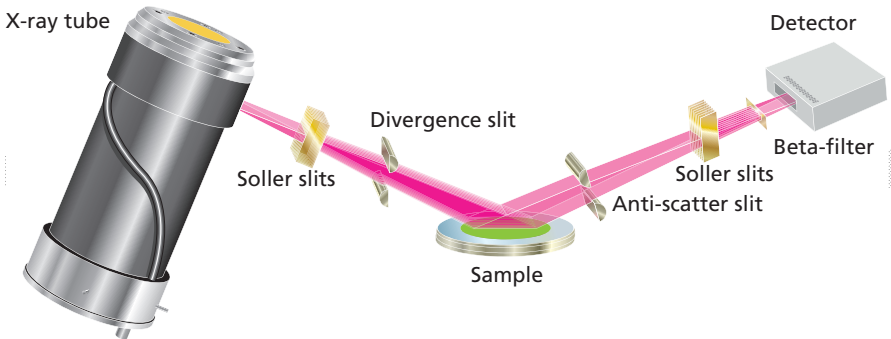


Figure 17. Classical powder diffractometer setup in Bragg-Brentano geometry with components for reflection measurements

Deviations in sample height lead to a shift of the position of the reflections. For example moving the sample upwards will shift the 2θ value of a particular reflection (see Figure 18) to higher angles.

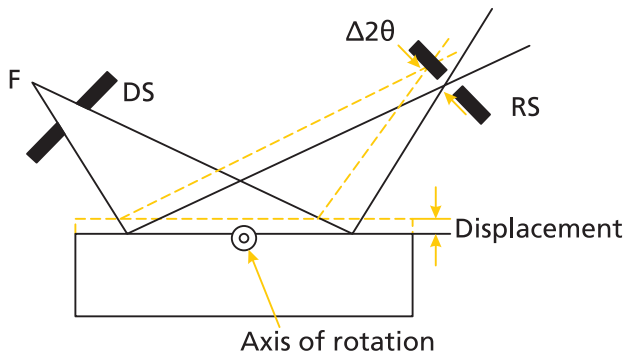


Figure 18. Effect of sample displacement with focusing geometry

In the Bragg-Brentano geometry, the diffracted angle is always twice the incident angle. In a traditional arrangement the diffractometer works in the $\theta/2\theta$ -mode, i.e. the tube is fixed and a 1:2 coupled movement of sample and detector is performed. Most current vertical diffractometers use the θ/θ -mode, where the sample always stays horizontal and tube and detector perform a 1:1 movement. This setup has some advantages:

- no powder spillage at high angles, even when spinning is used
- possibility to measure liquid or molten samples (non-ambient XRD)
- ability to measure very large samples on corresponding sample platforms or positioned not fixed to the goniometer

4.2.2 Transmission geometry

In order to realize a focusing setup in the transmission geometry, an additional focusing element is required between the X-ray source and the sample. This can be e.g. a focusing multilayer mirror or a focusing curved monochromator. The beam is focused through the sample on the (1D or line) detector.

Figure 19 shows a typical transmission beam path. The focus on the detector circle results in a very high resolution.

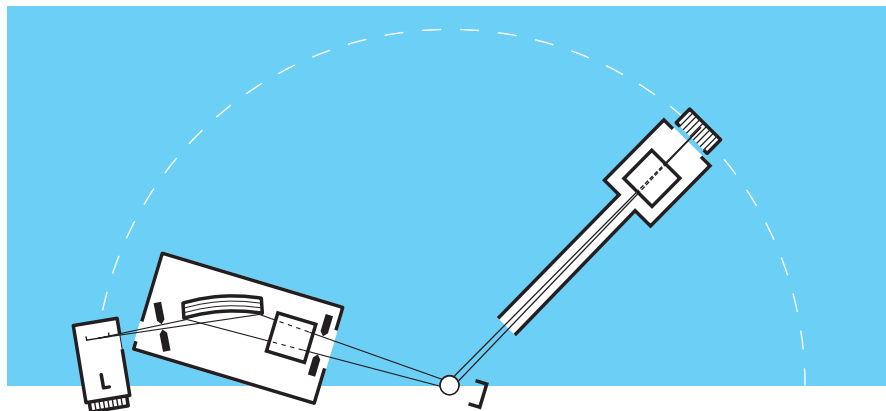


Figure 19. Sketch of typical transmission setup for capillary measurements, using focusing X-ray mirror and line detector

4.2.3 Parallel beam geometry

In a parallel beam geometry diffractometer (ideally equipped with an X-ray mirror and a parallel plate collimator), sample height variations do no longer influence the peak positions (see Figure 20). A disadvantage of this geometry is that a 1D position-sensitive detector can not be used.

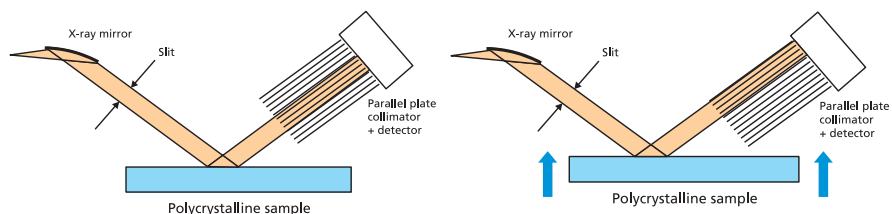


Figure 20. Parallel beam geometry and effect of sample height variation

4.2.4 Microspot analysis

Microdiffraction experiments require a small irradiated area. Special optics like mono-capillaries are used, together with e.g. a 1D or 2D detector like PIXcel^{3D}. This technique allows the investigation of sample areas less than 1 mm².

4.3 Optical components in the X-ray beam path

The optical path of a diffractometer can be divided in an incident and a diffracted beam path. These two different paths require different optical modules, depending on the technique and application. Typical optical components in the incident beam are divergence slits and mirrors, while in the diffracted beam path receiving slits and parallel plate collimators in combination with point detectors or position-sensitive detectors, sometimes in combination with monochromators, are used.

4.3.1 General requirements

The quality of an X-ray powder diffraction pattern is to a large extent determined by the choice of the optical components and their performance. Typically the following parameters are important for good quality diffractograms:

- high resolution of the reflections
- high intensity of the reflections
- low background

A standard Bragg-Brentano diffractometer is equipped with the following components for para-focusing geometry:

- Soller slits to define the axial divergence of the incident and diffracted beam
- primary divergence slit to define the illuminated length and mask to define the width of the beam
- β -filter and/or monochromator(s)
- receiving and anti-scatter slits in combination with point detectors, or
- anti-scatter slits in combination with position-sensitive detectors

Further optical options for specific applications with other than focusing geometry can be:

- multi-layer X-ray mirrors
- monocapillaries
- polycapillary lenses
- hybrid monochromators
- parallel plate collimators

A typical setup of a Bragg-Brentano diffractometer is shown in Figure 17.

4.3.2 Slit optics for Bragg-Brentano geometry

In a diffractometer the primary X-rays (emitted either from the line or point focus of the tube) have to be conditioned in a way that they just illuminate the sample. In a Bragg-Brentano setup the sample is illuminated by using a divergent

beam, defined by a divergence slit. The divergence is substantial for the focusing principle, so that the reflected beam from the lattice planes is focused on the receiving slit in front of the 0D or 1D detector. The distance between the focus and the sample is the same as between sample and receiving slit/1D detector.

4.3.2.1 *Divergence and anti-scatter slits*

Incident beam

The divergence slit settings have to be selected in a way that the illuminated area equals – but not exceeds – the sample size. This produces optimum intensities and prevents over-illumination. The use of smaller divergence slits leads to slightly sharper peaks, because flat samples do not allow perfect focusing (therefore called para-focusing geometry). On flat samples, the focusing condition is only valid in the middle of the sample. On the other hand, smaller divergence slits reduce intensity.

Diffracted beam

The anti-scatter slit assures that just the reflected beam and no air scatter reach the detector. The slit size corresponds to the divergence slit size. The anti-scatter slit is followed by the receiving slit. The receiving slit is placed at the focal point. The receiving slit size defines the resolution and the intensity. Smaller slits give higher resolution and lower intensity and vice versa. The size of the anti scatter slit has to match the size of the divergence slit to observe just the illuminated length. The receiving slit has to be set according to the resolution or intensity needed for the application.

Programmable slits

Programmable divergence and anti-scatter slits can be used both in fixed and in automatic/variable mode. The difference between the modes is:

- In fixed mode the length of the irradiated (and observed) area on the sample changes during a scan. The irradiated volume remains constant, the so-called measurement with constant sample volume.
- In automatic (or variable) mode the length of the irradiated (and observed) area on the sample does not change during a scan. The irradiated length remains constant, the so-called measurement with constant sample area.

The automatic divergence and anti-scatter slits of the X'Pert PRO and Empyrean diffractometers use two independently controlled knives and are controlled to assure symmetrical sample illumination even at very low angles.

The automatic anti-scatter slit on X'Pert PRO and Empyrean diffractometers provides additional functionality: together with a motorized receiving slit or a position-sensitive detector it can define a beam tunnel for reflectivity measurements, small-angle X-ray scattering or simple parallel-beam path applications.

Typical use of the different divergence slit modes:

Fixed mode:

for phase analysis and Rietveld (structure) refinement, because the diffractograms match the data of the ICDD database (see Chapter 6.2). The constant sample volume is a prerequisite for Rietveld analysis.

Automatic mode:

- for measurements at low angles to reduce the influence of primary beam scatter
- to improve the counting statistics at higher diffraction angles

In general, fixed slit intensities can be converted to variable slit intensities and vice versa with algorithms available in e.g. the HighScore phase analysis software.

Figure 21 demonstrates the change of the irradiated length with the 2θ angle for a range of slit sizes (from $1/32^\circ$ to 2°) and a measuring circle with $R = 240$ mm. Note that at low angles the illuminated length increases drastically.

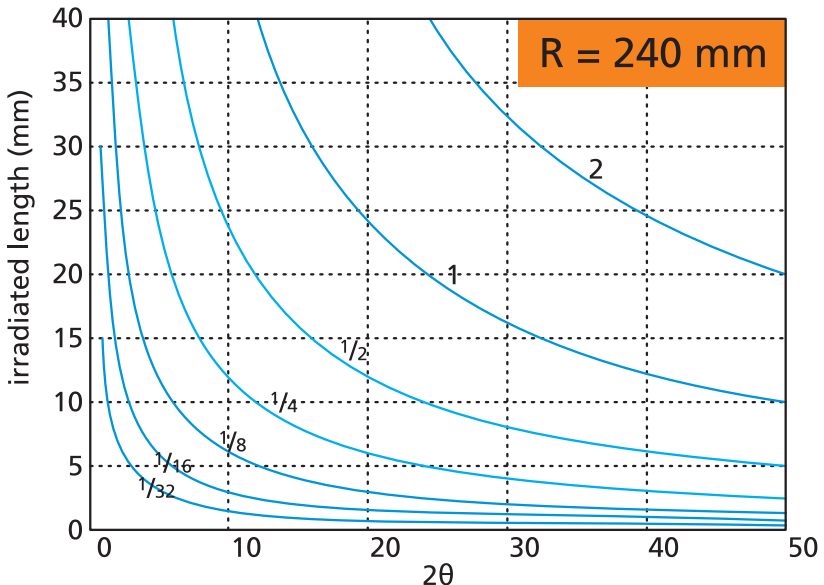


Figure 21. Slit divergence vs. irradiated length

4.3.2.2 Soller slits

Soller slits consist of a set of thin parallel metal plates. They can be placed in both the incident and the diffracted beam path. Only those parts of the beam which are parallel or very close to parallel to the diffraction plane can pass the Soller slit. Hence they limit the axial divergence of the incident and diffracted beam. The opening angle of a Soller slit is defined by the length and the distance of the plates. The typical Soller slit has an opening angle of 0.04 rad, but other sizes (0.08,

0.02 and 0.01 rad) are available. A smaller axial divergence improves the symmetry of the peaks, especially at low angles, as well as the resolution (smaller 'full width at half maximum', FWHM), but leads to lower intensities. The optimum choice depends on the required resolution and intensity.

4.3.3 Optical modules

In addition to slit systems there are other optical modules available for the incident and diffracted beam, which can be useful for several applications.

Task	Optical module(s) used
Suppression of unwanted wavelengths, for example white radiation or $K\alpha_2$	Primary or secondary monochromator, multi-layer mirror, filter
Parallel or focused beam	Mirror, collimator or lens
Increase of flux of the incident beam intensity	Mirror or lens
Reduction of beam size and/or intensity	Collimator/mask

$K\beta$ filter and monochromator

In order to obtain a good diffractogram it is important to reduce or eliminate the following unwanted effects:

- the $K\beta$ radiation
- the $K\alpha_2$ radiation
- the fluorescent radiation of the sample
- air scatter
- bremsstrahlung (tube background)

$K\beta$ filters are thin metal foils, which can be mounted in the primary or secondary beam path. They are usually used in the diffracted beam path to reduce the influence of sample fluorescence. The filter suppresses the beta emission line by utilizing the material-specific absorption edge. As shown in Figure 22, a Ni filter, used with Cu radiation absorbs >99% of the $K\beta$ part but also lowers the $K\alpha$ radiation by ~50%. Tungsten (W) L-lines, mainly present when using older tubes, are also suppressed.

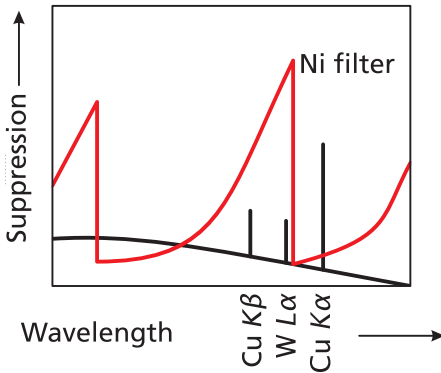


Figure 22. Absorption curve of a Ni filter (red)

The materials used as $K\beta$ filters are normally one atomic number below that of the anode material (Table 5).

Table 5. Relationship between anode and filter material

Anode material	$K\beta$ filter material
Cr	V
Fe	Mn
Co	Fe
Cu	Ni
Mo	Nb or Zr
Ag	Rh or Pd

When using X-ray mirrors or primary monochromators, the use of a β filter is not necessary, since $K\beta$ is completely suppressed by these optics.

Primary monochromators consist of one or more single crystals. They are positioned in the beam path in such a way that the incident beam on the lattice plane fulfills the Bragg equation (see Chapter 3.5.2). Since the Bragg equation is only valid for specific wavelengths at a given angle, the diffracted beam from the crystal is highly monochromatic. The use of a monochromator always leads to a lower primary beam intensity, because only a part of the wavelengths is used and intensity is absorbed in the monochromator crystal. The combination of several adjacent crystals improves the spectral purity of the incident beam but leads to additional attenuation of the intensity.

Secondary beam monochromators consist either of a flat or a curved single crystal. The commonly used single monochromator in the diffracted beam behind the receiving slit eliminates the $K\beta$ radiation, but the complete $K\alpha$ doublet passes to the detector.

Figure 23 shows the beam path when using an incident beam monochromator in reflection mode. The curved incident beam monochromator is aligned in a way that just the $K\alpha_1$ wavelength passes the divergence slit. Fluorescent radiation of the sample is not eliminated, but the monochromator reduces this effect, because now only the $K\alpha_1$ component can excite the fluorescence. $K\beta$ and white radiation are not present any more. If necessary, an additional secondary monochromator can be used for further suppression of fluorescent radiation.

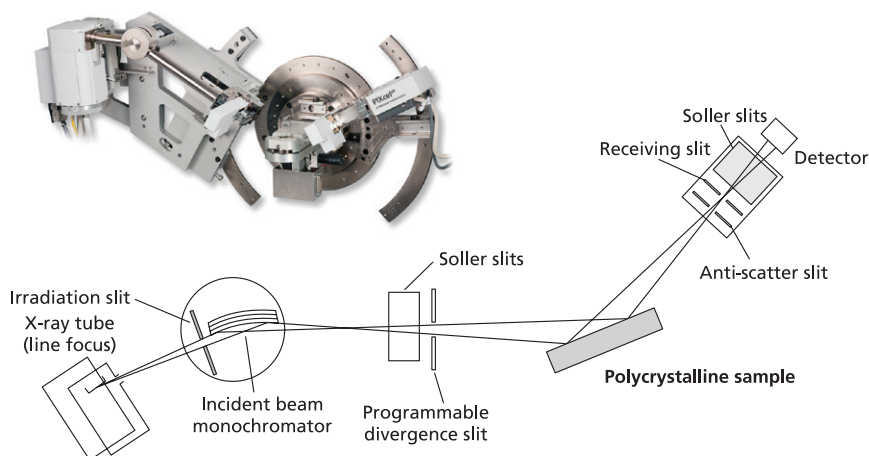


Figure 23. Beam path and example picture of Alpha-1 Bragg-Brentano diffractometer

4.4 Detectors

4.4.1 General remarks

X-ray detectors can be classified in three different types:

Point or 0D detector	All incoming photons are counted, their position on the active element is not relevant.
Line or 1D detector	Also called position-sensitive detector, i.e. photons are counted relative to their position on the detector window in 2θ direction.
Area or 2D detector	Similar to the line detectors, but intensities are also detected perpendicular to 2θ axis.

Application-specific requirements

The table below lists all the properties that are of importance for a detector used in X-ray diffraction:

Property	Description
<i>Angular resolution</i>	The ability of the detection system to distinguish between different d -spacings (the ability to separate neighboring reflections). Mainly defined by slits in front of a point detector or the width of the channels of a position-sensitive detector.
<i>Energy resolution</i>	The ability of the detection system to detect only $K\alpha$ or $K\alpha_1$ radiation and suppress unwanted radiation (for example: $K\beta$ or sample fluorescence). The point and line detectors incorporate electronics that allow using a (variable) pulse height discrimination, which acts like a band pass filter. The energy resolution of such a filtering is usually moderate, so that additional means of energy filtering such as $K\beta$ filters or diffracted beam monochromators have to be used.
<i>Count rate linearity</i>	The intensity at which the recorded intensity starts to deviate more than 5% from the incident intensity, above this value, the deviation will become larger until the detector finally saturates. In extreme cases this leads to untypical peak shapes with a minimum at the peak tip position.
<i>Detector noise</i>	The noise level of a detector, in most cases $\ll 1$ cps.
<i>Dynamic range</i>	The counting range of a detector, defined as the difference between noise level and the highest intensity possible without saturation.
<i>Measurement time</i>	The time that the detector needs to measure a certain angular range.
<i>Possibility for in-situ measurements</i>	Determination of changes in the sample as a function of an external parameter or time, for example: temperature-controlled experiments, humidity, crystallization and so on.
<i>Active length or active area</i>	The angular range that is covered by a line detector or the size of the detecting element of a point detector (important for grazing incidence or parallel beam experiments).

What a detector really sees

In a polycrystalline material all reflected beams coming from a certain lattice plane (with a certain d -spacing) form the Debye-Scherrer 'cones', centered around the incident beam.

Figure 24 helps to understand this principle. With a standard diffraction system using slits or line detectors just a part of that cone is used for the measurement because point and line detectors measure just one segment of the Debye-Scherrer rings (yellow lines). This is partly compensated by using the line focus of the X-ray tube together with Soller slits. In this case many parallel incident beams hit the sample so that the recorded signal consists of the overlapping tops of the diffraction rings of the same d -value.

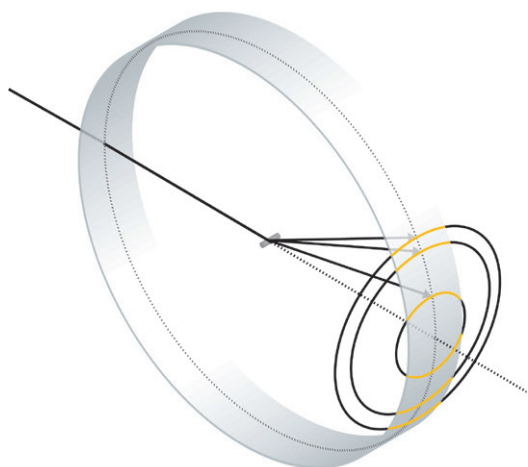


Figure 24. Debye-Scherrer setup with some diffraction cones

4.4.2 Detector types

In modern powder diffractometers different types of detectors can be used, depending on the application. In the following the most common types are presented.

Point detectors

Two types of point detectors are widely used for almost all diffraction applications: gas-filled proportional counters and scintillation counters. The selection of the appropriate detector heavily depends on the choice of tube anode material.

Gas proportional counter

Gas-filled proportional counters consist of a metal cylinder with an entrance window for X-ray photons. The cylinder is cross-sectioned by a thin wire attached to a high-voltage positive potential. The detector is filled with a noble gas, either argon or xenon. The incoming X-ray photon ionizes the atoms of the counting

gas. The ionization electrons are accelerated to the wire and are ionizing further atoms (charge avalanche). At the counting wire an impulse with an amplitude proportional to the energy of the absorbed X-ray photon is generated and recorded by a pulse-height discriminator.

This detector type is the optimum choice for standard wavelengths as Cu $K\alpha$, Co $K\alpha$, and Cr $K\alpha$ radiation. The detector has a very low background and a good energy resolution.

Scintillation counter

Scintillation counters consist of a crystal and a photomultiplier. The crystal is capable to convert an X-ray photon into a UV or visible photon. The incoming X-ray photon is absorbed in the crystal (for example: NaI, doped with Tl). The resulting light impulse is recorded by the photomultiplier as an amplitude proportional to the energy of the absorbed X-ray photon. Scintillation detectors have a lower energy resolution than gas proportional counters for Cu $K\alpha$ radiation. However, they are preferred for short wavelengths (e.g. Mo $K\alpha$ or Ag $K\alpha$).

The main properties of point detectors regarding their applications are

- high dynamical range ($\sim 10^6$)
- possibility to use a diffracted beam monochromator
- low (background) noise
- can be used with focusing or parallel beam geometry
- cost-effective

Line detectors

Line detectors cover a certain angular range in 2θ . They resemble a large number of adjacent single detectors. Line detectors are thus much faster than point detectors. Different types are on the market. The first commercial line detectors used a wire and a counting gas. Since 2001 semiconductor detectors define the new standard. The PANalytical X'Celerator with its unique semiconductor RMTS (Real Time Multiple Strip) technology was the first detector of that kind on the market. The X'Celerator overcame the problems of the gas-filled detectors, which have a small dynamic range and need regular maintenance because of aging of counting gas and detector wires. The current state-of-the-art PANalytical PIXcel^{3D} detector consists of smaller strips than the X'Celerator. The strips are subdivided in segments so that the PIXcel resembles a solid-state area detector. It has a better resolution and the highest linearity of all detectors available for laboratory XRD equipment. The detector can be used in point detection mode, in line detection mode and as an area detector. This makes it also the ideal detector for measurements of epitaxial layers, reflectometry and small-angle X-ray scattering, which require a very large dynamic range. Secondary monochromators are exclusively available for these detectors, to improve energy resolution and suppress sample fluorescence.

Most line detectors have an active length of a few degrees so that the deviations from the ideal focusing geometry are not too large. The use as a scanning detector further reduces this defocusing effect. Line detectors are primarily designed for focusing geometry, but can also be used with parallel beam geometry in reflection

or transmission. In order to maintain an acceptable resolution in these cases, the width of the beam has to be small.

The main properties of line detectors regarding their applications are:

- very fast measurements and/or improvement of counting statistics
- investigation of time-resolved processes
- small sample amounts and areas can be investigated
- excellent angular resolution (in case of solid-state types)
- outstanding linearity (in case of PIXcel)

Area detectors

Area detectors can record larger parts of the Debye rings or even complete rings at low angles. They are suited for special applications like micro-diffraction and texture analysis. They are also widely used for single crystal diffraction. Different designs are on the market.

The main properties of area detectors in powder diffraction are

- very fast measurements and/or improvement of counting statistics
- usage of a bigger part of the Debye-Scherrer rings, which allows analysis of small spots (micro-diffraction) and small sample quantities.
- improved analysis of highly textured samples
- resolution sometimes less than with line detectors, but solid-state detector like PIXcel^{3D} without compromise

4.4.3 Comparison of the detector types

Properties:	Point detector	Line detector	Area detector
Irradiated area	From large to small	From large to small	Small
Sample information	Integral	Integral	Small spot (micro-diffraction)
Influence of preferred orientation and grain size effects	Not directly visible	Not directly visible	Directly visible (spotty rings)
Angular resolution	Excellent	Excellent	Moderate to excellent
Data recording speed	Low	High	High
Energy resolution	Very high	High	Low to high
Linearity	High	High to very high	Moderate to very high

Application areas of the different detector types:

Application	Point detector	Line detector	Area detector
Phase identification	Yes	Yes	Yes
Quantification based on one or a few peaks	Yes	Yes	Yes
Quantification based on full pattern analysis	Yes, but slow	Yes	Yes
Residual stress	Yes (especially with parallel beam geometry)	Yes	Yes
Texture	Yes	Yes	Yes
Micro-diffraction	Yes, but slow	Yes	Yes
Reflectivity	Yes	Yes	No



PANalytical



PANalytical



PANalytical

5. XRD data collection

5.1 Sample preparation

General remarks

- ensure that the sample is representative
- do not treat the original sample more than necessary
- if milling is required, be as careful as possible
- select the best measuring geometry depending on the sample and the information needed
- in reflection mode θ/θ setup is preferred.

5.1.1 Ideal powder

The ideal powder has no internal stress and has no crystallographic preferred orientations. The optimal particle size of powder diffraction samples is in the range of 1 to 5 μm .

If the powder is too coarse this results in single points on the Debye-Scherrer ring. Therefore point or line detectors do not recognize all reflections which leads to incorrect intensity ratios.

If crystallites are much smaller than 1 μm , reflections are broadened. This effect can be used for crystallite size determination, see Chapter 9.3.

Table 6 shows some of the possibilities and risks involved in the milling process.

Table 6. *Milling processes, their possible problems and remedies*

Problem	Possible consequences	Possible remedy
Heating of the powder	– phase transitions – oxidation	use easily vaporizable liquids (for example: acetone)
Plate-like materials (for example Mica)	– mills very badly – texture effects	use liquid N_2 to make the material brittle
Too long grinding	– destruction of crystal lattice – sample becomes amorphous	grind no longer than necessary
Inhomogeneous mixtures	The sample can be a mixture of hard and soft material and is therefore more difficult to treat	

5.1.2 Sample types

The different X-ray powder diffraction techniques can investigate all kinds of samples and sample shapes. These include bulk materials and powders, wafers and thin layers, gels and liquids, polished and rough surfaces, very small quantities, and air- or humidity-sensitive materials.

Figure 25 to Figure 27 show different sample holders for reflection, transmission and capillary measurements.

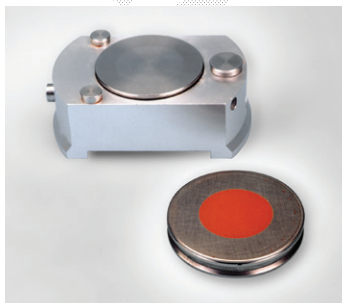


Figure 25. Sample holder for reflection measurements



Figure 26. Sample holder for transmission measurements



Figure 27. Capillary sample mounted on goniometer head

5.1.3 Reflection mode

In reflection geometry the surface of the samples should fit the focusing circle of the instrument as best as possible to prevent peak shifts. Polished and rough surfaces may be investigated as well as gels or liquids. On rough samples, a parallel beam geometry is preferable.

The sample is often rotated (sample spinning) to improve the particle statistics.

Especially for small-angle diffraction a knife edge (sometimes called a beam knife) close to the surface of the sample is useful to reduce the background produced by air scattering.

Bulk materials / powders

Make sure that the surface of the sample is at the correct height in the center of the measuring circle.

Gels, liquids and loose powders

The θ/θ geometry is the preferable arrangement, since the sample always stays horizontal. In a $\theta/2\theta$ diffractometer the incident beam angle ω needs to be fixed so that the sample does not spill; this technique however can cause peak broadening and peak shifts.

5.1.4 Foil transmission

For transmission measurements the absorption of the material plays an important role. Generally, the ratio of the incident beam intensity I_0 and the transmitted intensity I of the sample should not exceed a factor of 3 to 4. The usable sample thickness depends on the sample itself, ranging from several micrometers for highly absorbing material up to 3 or 4 mm thick pharmaceutical tablets.

Powders

Powdered samples are placed between two thin foils (e.g. Kapton or Mylar).

Bulk materials and foils

As long as absorption is not too high, bulk samples can be placed directly in the sample holder.

Gels / liquids

A special sample holder is needed to fix the material in a special small chamber.

5.1.5 Capillaries

Powder samples sensitive to moisture or texture effects are ideally analyzed in capillaries. The powder is loosely filled into the capillary without application of pressure.

The X-ray transparency in the capillary may be improved by diluting the sample with amorphous substances, for example cork flour, glass and/or lycopodium.

Powders

The material is filled in 0.1 to 2 mm thick capillaries. The capillary diameter is selected depending on the grain size and the X-ray transparency.

Gels / liquids

These materials can be prepared into a thicker capillary. Alternatively, the material can be spread onto the surface of the capillary.

5.2 Measurements

5.2.1 Optimum measurement conditions

Reflection mode

In general a coupled movement of the scan axes ($\theta/2\theta$ or θ/θ) is used (Bragg-Brentano geometry). Other movement modes are possible, depending on the application (e.g. fixed ω for grazing incidence measurements of thin layers or $\omega=0$ for SAXS experiments). Variable or fixed slit settings can be used (see Chapter 4.3.2). Sample spinning improves the particle (crystallite) statistics.

Foil transmission

The maximum sample thickness depends on the sample material. For successful transmission experiments the sample should have a low mass. When investigating thick samples (e.g. a 3 mm pharmaceutical tablet) the sample is normally rotated (spun) to improve the particle statistics and the center of the sample should be at the center of the rotation in ω . In general sample spinning improves the particle (crystallite) statistics.

In addition to sample spinning, tilting the sample in $\pm \omega$ (wobbled scan) further reduces the effect of preferred orientation.

Capillary

The capillary is fixed on a goniometer head and adjusted using a microscope or CCD camera (Figure 27).

The incident beam is collimated so that it matches the diameter of the capillary as good as possible. This will reduce air scattering to a minimum and will lead to a low background at low angles. The ω angle is fixed at zero and the detector moves on the 2θ circle. The capillary rotation decreases the influence of preferred orientations.

5.2.2 Resolution

The resolution of a diffractometer is defined by its ability to differentiate neighboring reflections (see Chapter 3.7). In order to obtain an optimal resolution, different geometries with certain properties can be used. The maximum achievable is the

sum of the properties of the sample and the diffractometer, i.e. X-ray tube, goniometer radius, incident and diffracted beam optics and detector.

General remarks

Assuming that the sample is fine-grained (see Chapter 4.3.1), unstressed and without lattice dislocations, the resolution will be improved by

- increasing the radius of the measuring circle
- using pure $K\alpha_1$ radiation instead of the $K\alpha_{1,2}$ doublet
- using longer wavelengths
- using smaller Soller slits
- using narrower slit widths:

The divergence slit and Soller slit have a substantial effect on the attainable half widths of reflections. This is particularly true for the Soller slits when you consider how they determine the cutout from the Debye-Scherrer cone in the plane of measurement.

- making the sample as thin as possible. For

reflection	fine powder on zero background holder
foil transmission	low amount of powder between the foils
capillary	smallest as possible diameter.

Small step sizes in 2θ are necessary when measuring peaks with a small FWHM (at least five measurement points over the FWHM are required).

In general:

1. A compromise is often necessary, because the possibilities shown here usually result in a decrease of the measured intensity.
2. With a standard setup FWHMs of approximately $\Delta 2\theta = 0.06^\circ$ to 0.12° over the whole angular range can be achieved. Higher resolution is possible using different measurement strategies and optimized setup.

5.2.3 Low quantities

The analysis of low quantities usually leads to problems with limits of detection (LOD) or limits of quantification (LOQ) (see Chapter 7.2.3).

For best results the incident beam should illuminate as many sample particles as possible, so careful selection and setup of primary and secondary optics is necessary. It may be helpful to perform the measurement without spinning the sample, when particles do not stick to the sample holder.

Remark: If a sample is visible and can be prepared, a useable diffractogram can be expected.

Reflection mode

The substances should be fixed on a 'zero-background holder' (e.g. silicon (510) or (511) oriented or quartz (6° offcut to c axis)). Also an amorphous substrate such as glass can be used, but it leads to higher undesired background.

Alternatively the sample can be mounted on a special micro-diffraction stage, which uses a goniometer head for positioning and spinning.

Foil transmission

A small amount of the sample material should be carefully placed between the two foils. Using a smaller beam mask helps to reduce air scattering.

Capillary

The amount of material in the capillary should be sufficiently illuminated by the primary beam. If the amount of sample material is insufficient to entirely fill the capillary one can partially fill it with a supporting substance and subsequently with the sample so that the sample material is placed in the X-ray beam. Alternatively the material itself can be diluted with a reflection-free powder (cork powder, glass and/or lycopodium) to increase the total sample volume.

5.2.4 Air-sensitive / hygroscopic materials

For the analysis of air-sensitive/hygroscopic samples the preparation should be done immediately before the measurement starts. The measurement must be performed as quickly as possible and low counting statistics have to be expected. Note, that the diffractogram may represent different substances at low and at high 2θ angles, e.g. different hydrates, depending on the reaction rate of the sample with air or moisture.

Reflection mode

The sample is prepared in a special sample holder that can be covered with a foil.

Foil transmission

Prepare the sample between foils, or, if it is thick enough, in a closed sample holder (only for low absorbing materials).

Capillary

The use of a sealed capillary is usually the best choice when investigating air-sensitive or hygroscopic materials.

5.2.5 Minimization of texture

Minimizing the effect of preferred orientation(s) and texture is a task to overcome one of the main problems in qualitative and quantitative phase analysis, see Figure 28.

Rotating (spinning) the sample only improves the particle statistics. The influence of preferred orientations may be reduced by oscillating the sample in an additional direction, for example: $\pm \Delta\omega$ (wobbled scan).

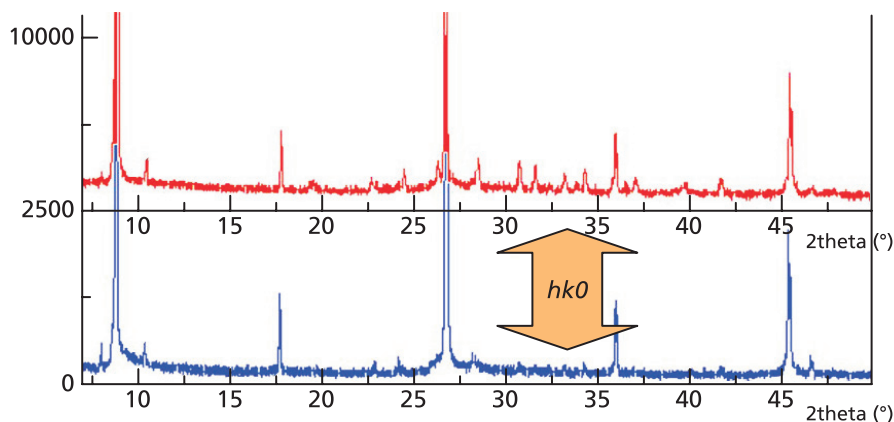


Figure 28. Texture effect through different sample preparation, resulting in missing peaks

Reflection mode

Texture problems are mostly visible when using reflection geometry.

Preferred orientation caused by the preparation of powder measurements can be minimized by

- avoiding smoothing of the surface in one direction
- back-loading of the sample into the sample holder
- filling the powder against a lateral glass plate
- roughing the surface
- spray-drying the sample on a plate

Note: for clay mineral analysis, texture is sometimes desired to study the swelling of minerals (determination of moisture absorption) or to simplify the phase analysis. A special preparation method is used to maximize the preferred orientation of the platy clay minerals. This method pronounces the (00l) reflection and allows a better peak position determination (see also Figure 28).

Transmission mode

To enhance the (hk0) reflections, an additional movement of the sample in $\pm \Delta\omega$ can help to decrease a texture regarding the (00l) reflections. The influence of preferred orientation is significantly reduced.

Capillary

The investigation of loosely filled powders in capillaries is clearly advantageous to overcome the texture problem. Both the rotation of the capillary and the possible movement of the particles inside the capillary reduce texture effects.

If needle-shaped crystals have to be investigated, putting them into a capillary is the preferred way of preparation. Furthermore it eradicates the need for any further handling such as grinding.

5.2.6 Thin layers

Thin layers are often defined differently. 'Thin' can mean several micrometers, which can be for example a corrosion layer on a metal or can be a few nanometers as a coating on glass. The penetration depth, dependent on material, wavelength and incidence angle, can be just a few microns, so 'thin' means sub-micron range down to several nanometers. The material can be everything from single crystal to amorphous. The investigation is normally performed using reflection geometry. Only in a few cases the film can be detached from the substrate and then measured in transmission mode.

In thin film experiments the intensity of the layer peaks is not comparable to the intensity we get from powder samples, because the number of reflecting lattice planes is much less. Besides that the sample is not infinitely thick. This requires a special beam path to optimize the intensities. Two options are widely used:

1. Usage of parallel beam geometry with grazing incidence of the primary beam. The sample surface is completely irradiated over the full angular range. Furthermore the grazing incidence beam is not diffracted by the substrate so that strong substrate signals are suppressed.
2. If parallel beam geometry cannot be used, it helps to use programmable slits in the primary beam, set to a fixed illuminated length to keep the irradiated area and therefore the sample volume of the layer constant.

Table 7 shows how the penetration depth changes by varying the incident angle ω and the wavelength (λ). A brass sample (layer) is used as an example. A penetration depth $d_{86.5}$ (delivering 86.5% of the information) is calculated. It can be clearly seen that the penetration depth can vary between 9.67 μm and 0.25 μm by changing from Mo $K\alpha$, radiation with a 'normal' incident angle of 25° to Cr $K\alpha$ with an ω of 1.0°.

Table 7. Influence of the used wavelength and the variation of the incident angle ω on penetration depth

Sample: Brass (30 at.% Zn), for effective penetration depth $d_{86.5}$ (in μm)

Radiation	μ/cm^{-1} ω :	25°	10°	5°	3°	2°	1°
Cr $K\alpha$	1351	3.11	1.58	1.01	0.66	0.46	0.25
Co $K\alpha$	705	6.00	3.05	1.93	1.27	0.90	0.47
Mo $K\alpha$	434	9.67	4.93	3.13	2.07	1.43	0.78

Remark: It may be advantageous to use a wavelength with a high absorption to make sure that only the sample surface is investigated, for example Cr or Cu radiation to investigate steel surfaces.

5.2.7 Rough surfaces

Rough surfaces (rocks, porous substances, etc.) are usually measured in reflection geometry. The best primary optic is a parabolic X-ray mirror that produces a parallel beam. To collect the diffracted intensity of a parallel beam a parallel plate collimator or a diffracted beam mirror is needed between sample and detector (see also Figure 20).

5.2.8 Standard materials

Validating a powder diffractometer to check the performance requires the use of certified materials, called standards. This is especially important in regulated environments such as those encountered in the pharmaceutical industry. Standards should be stable over a period of time and be easy to prepare for use in the diffractometer.

The most regularly used standards come from the US National Institute for Standards and Technology (NIST). Their Standard Reference Materials (SRMs) are listed in Table 8.

Table 8. Standard materials for XRD as supplied by NIST (main application field marked (x)).

SRM no.	Type	Application				
		Reflection position	Intensities	Profile	Quantitative phase analysis	Lattice parameters
640d	Si	X	X	X		X
660b	LaB ₆	X	X	X		X
675	Mica	low angles				
656	Si ₃ N ₄ (mixture α/β)				X	
674b	Mixture Al ₂ O ₃ , CeO ₂ , Cr ₂ O ₃ , TiO ₂ , ZnO				X	
676a	Al ₂ O ₃ powder		X		spiking method	
1878a	Respirable α quartz		X		spiking method	
1879a	Respirable cristobalite				spiking method	
2910a	Ca-hydroxyapatite		X	X		X
1976b	Al ₂ O ₃ disk		X	X		X

Currently, there is no NIST certified standard for powder diffraction at low angles. Nevertheless silver behenate ($\text{CH}_3(\text{CH}_2)_{20}\text{COOAg}$) (reference to Powder Diffr. 10 (1995) 91) is widely used for this purpose.



PANalytical



PANalytical



PANalytical



PANalytical



PANalytical

6. Qualitative phase analysis

There is a large variety of information that can be extracted from a powder diffractogram. In this chapter, most attention is paid to one of the most common types of analysis: the qualitative analysis of mixtures.

6.1 Data processing

The diffraction pattern (intensity I versus Bragg angle 2θ) is characteristic for each crystalline substance, and its crystal structure is represented in the position and the intensity of the reflections. Also, substances with the same chemical composition, but different crystal structure (for example TiO_2 , modifications rutile/ anatase/ brookite) differ in their structure and hence in their diffractograms.

The typical sequence of a phase analysis is:

1. A visual inspection of the diffractogram (peak positions, intensities, peak widths and background shape).
2. Start of a peak search algorithm to get the positions and both absolute and relative maximum intensities of the reflections. The strongest line is normalized to 100% (see Table 9).
3. If necessary (graphical) editing of the peak table.

Table 9. A typical peak list

Nr.	Position [$^{\circ}2\theta$]	d -value [Å]	Rel. intensity [%]	Intensity (cts)
1	8.1061	10.9074	14.21	648.14
2	16.2197	5.46486	2.13	97.1
3	24.4002	3.64808	1.17	53.19
4	29.4716	3.03086	4.32	196.96
5	33.7833	2.65325	21.43	977.14
6	38.1742	2.35757	100.00	4560.28
7	39.0926	2.30427	10.73	489.48
8	39.4911	2.28194	59.08	2694.4
9	41.7069	2.16568	2.35	106.96
10	45.8081	1.98088	1.48	67.67
11	49.9124	1.82719	1.89	86.06
12	51.0983	1.78753	0.48	21.91
13	55.0748	1.66751	23.3	1062.53
14	55.7635	1.64854	2.65	121.04
15	57.7995	1.59522	0.81	37.04
16	58.9689	1.56635	1.79	81.54
17	61.4021	1.50999	0.28	12.97
18	63.6738	1.46148	0.88	40.33
19	64.5270	1.44421	3.31	150.81
20	66.1805	1.41208	5.40	246.21
21	69.8449	1.34669	23.11	1053.92
22	72.4648	1.30433	3.59	163.69
23	77.5035	1.23163	1.63	74.37
24	81.6514	1.17924	5.03	229.27
25	84.9777	1.14137	2.08	94.96
26	89.9543	1.0907	1.53	69.73

Such a peak table can be used for the search/match procedure. Better intensities and peak positions are obtained after a profile fitting step has been applied, but this is not crucial for a correct phase analysis.

Different software routines like for example available in the HighScore software package allow automatic processing of data, using user-defined parameter sets, even including reporting to either a printer or a laboratory information management system (LIMS), as well as trend analysis.

6.2 The search/match procedure; reference databases

In this procedure, the measured diffractogram (with its peak table and/or profile) is compared with a reference database consisting of experimentally determined d -values and intensities (d - I tables or stick patterns) or of calculated

patterns from crystal structure data. Such a reference database is provided by the ICDD (International Centre for Diffraction Data), which supplies the PDF database (Powder Diffraction File, in former times named ASTM and JCPDS). It is annually extended with a set of new, experimentally determined reference patterns. New phases are included in the PDF database after passing an extensive editorial process. Older data (from films) are more and more replaced by digital measurements.

Since 1998 the database also contains calculated stick patterns, taken from databases containing crystal structure information, for example: the ICSD (Inorganic Crystal Structure Data Base) and the LPF (Linus Pauling File). In some cases, not only the stick patterns but also the structures themselves are incorporated in the PDF database. This extends the possibilities to perform certain types of quantitative analyses directly, such as the Rietveld analysis.

ICDD reference databases

PDF-2	Experimentally determined stick patterns and calculated patterns taken from the ICSD database
PDF-4+	PDF-2 plus calculated stick patterns and structure data from the LPF
PDF-4/Organics	Calculated stick patterns from the CSD (Cambridge Structure Database) and experimentally determined patterns relevant for pharmaceutical research (taken from the PDF-2)
PDF-4/Minerals	Subfile of PDF4+, containing mineral phases only

Recently also alternative databases have been developed, ranging from freely downloadable ones calculated from crystal structures, to speciality databases for niche fields, such as narcotics.

6.3 Cluster analysis

Cluster analysis is a multi-variate statistical method. It greatly simplifies the analysis of large amounts of data. It automatically sorts closely related scans of an experiment into separate clusters and marks the most representative scan of each cluster as well as the most different patterns of one cluster. It is very useful for e.g. non-ambient studies, control of syntheses or for example zeolites and pharmaceuticals, to find polymorphs and solvates in drug development and many other experiments consisting of a large number of measurements.

Cluster analysis is basically a three step process, but can also include an optional fourth step:

1. Comparison of all scans with each other. The result is a correlation matrix representing the similarity of any given pair of scans.

2. Agglomerative hierarchical cluster analysis puts the scans in different classes defined by their similarity. The output of this step is displayed as a dendrogram, where each scan starts at the left side as a separate cluster, and these clusters amalgamate in a stepwise fashion until they are all united.
3. The number of clusters is estimated by the KGS test (L.A. KELLEY, S.P. GARDNER, M.J. SUTCLIFFE) or by the largest relative step on the dissimilarity scale. Also the most representative scan within each cluster is determined.
4. PCA (principal components analysis) can be carried out as a separate and independent method to visualize and to judge the quality of the clustering. The correlation matrix of step 1 is used as input.

Additionally there are cluster validation techniques like silhouettes or fuzzy clustering available. It is also possible to connect additional properties to the cluster analysis, for example the temperature. Even different analyses like NMR or Raman spectroscopy can be clustered together with XRD scans.



7. Quantitative phase analysis

This chapter is designed to provide a brief introduction of using XRD measurements for quantitative analysis.

7.1 Basics

The fundamental condition of the quantitative phase analysis is that the intensity of the X-rays diffracted by a certain phase is proportional to its amount in the phase mixture (*H.P. KLUG and L.E. ALEXANDER*).

The following equations refer to the investigation of crystalline phases. The samples are powder mixtures in the sense of the statistical demands. The conditions for the application of the kinematic theory must be fulfilled.

The intensity I_{hkl} of a reflection is given by:

$$I_{\text{hkl}} = K_0 a \left(\frac{|F_{\text{hkl}}|}{V_{\text{uc}}} \right)^2 H P L$$

with

- a absorption coefficient
- H multiplicity factor
- P polarisation factor
- L Lorentz factor
- V_{uc} volume of the unit cell
- K_0 constant for the equipment:

$$K_0 = \frac{I_0 e^4 \lambda^3 Q_0}{m_e^2 c^4}$$

with

- I_0 intensity of incident or primary beam
- e elementary charge
- λ used wavelength
- Q_0 cross section of the incident beam
- m_e mass of the electron
- c light velocity

F_{hkl} structure amplitude:

$$F_{\text{hkl}} = \sum f_j e^{-M} e^{2\pi i(hx_j + ky_j + lz_j)}$$

with

- f_j scattering factor of each atom j
- e^{-M} temperature factor
- h, k, l Miller indices
- x, y, z coordinates of the atoms

To the percentages by volume v_k of the individual phases k in a mixture applies their diffracted intensity I_k :

$$I_k = K_0 R_k A_k V_k$$

provided that $\sum v_k = 1$.

The *absorption coefficient* A_k can be set $\frac{1}{2}\mu_k$, whereby the *attenuation coefficient* μ_k has to be possibly modified for a phase k in the mixture with other phases (then named μ_k').

General remarks

Quantitative phase analysis is usually implemented automatically using calibrations or the Rietveld method. Some fundamental requirements should be met in order to get the most reliable results.

- Use the integral intensities of the reflections.
- Use as many reflections as possible, but with different indices. Reflections with the same indices may falsify the result, if they present a preferred orientation (e.g. 220 and 440 reflection).
- Take into account a possible influence of the absorption contrast, also called micro-absorption, especially if a spiking material has to be selected.
- Take care of the influences of texture through careful milling and/or sample preparation and sample movements (at least spinning) during the measurement in an optimal measuring geometry.
- Check the reproducibility of the quantitative result by repeating the experiment a couple of times, preferably with a complete new preparation and handling, or even the use of automatic sample preparation equipment in order to eliminate operator dependencies.
- Double-check critical results by validation with an alternative technique, for example: X-ray fluorescence, cathodoluminescence or another microscopic method.

The following chapters describe possible ways of carrying out a quantitative phase analysis with respect to the sample possibilities, attenuation effects, micro-absorption, preferred orientations, automated procedures and amorphous contents, from classical methods up to the Rietveld method.

7.2 Special problems

7.2.1 Preferred orientation

Preferred orientation (unwanted texture) is usually the main problem for any quantitative phase analysis. For bulk solid materials there is no solution to avoid preferred orientation. For powder samples, one can reduce the influence of preferred orientations by a careful preparation or choosing different measurement parameters or diffraction geometries (e.g. wobbled scans or transmission diffraction).

Preparation

The sample is milled until the ideal particle sizes of 1 to 5 μm are achieved. Because the preparation effect is especially important for reflection mode measurements, the preparation problems are described in Chapter 5.1.

Measurement

Figure 29 shows the measurements of a mica sample in three measurement modes.

With regard to the reflection intensities it becomes clear that

- the reflection geometry enhances the (00l)-reflections
- the foil transmission reduces the (00l)-reflections in favor of the (hk0)-reflections
- the capillary measurement delivers the optimum result.

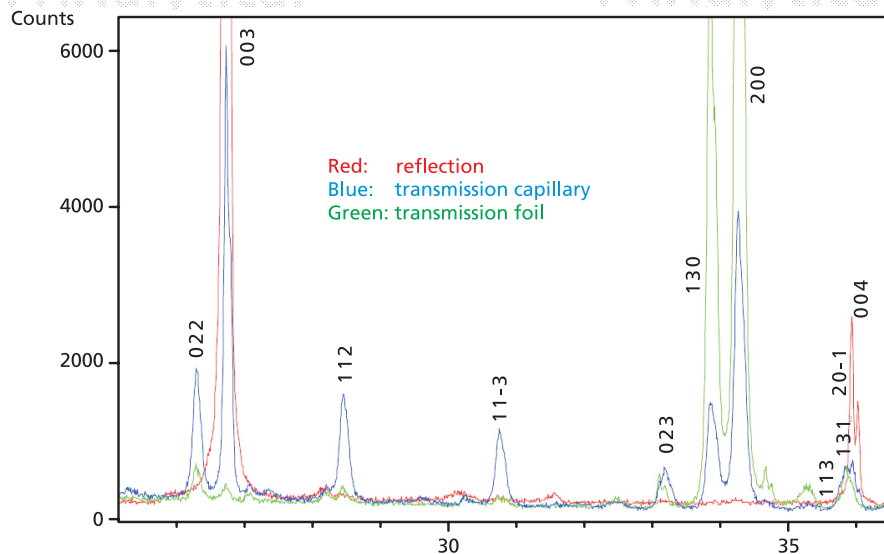


Figure 29. Comparison of mica diffractograms in different measurement modes

The rotation of the sample (spinning) may be one way to reduce the preferred orientations, but in reflection and foil transmission mode it mainly increases the particle statistics. A more effective way is an additional small oscillation of the sample holder, i.e. adding up different scans performed with different ω offsets (wobbled scan).

7.2.2 Absorption and micro-absorption

Absorption

Absorption effects may influence the results of quantitative phase analyses in a significant way. The absolute intensity of a diffraction peak will be proportional to the number of diffracting lattice planes. The Bragg-Brentano geometry with fixed divergence slit setting corresponds to the *ideal* case where the irradiated volume of the specimen stays constant at all diffraction angles, because of smaller surface areas combined with higher penetration depths at increasing angles. Thus, to account for the effect of specimen absorption on the diffracted intensities, the intensity equation only requires a constant factor $\frac{1}{2}\mu$ (see Chapter 7.1).

Micro-absorption

If a sample contains particles of different sizes, there is a significant effect on the resulting intensities, because the size of the particle corresponds to the absorption factor (the bigger the particles the higher the absorption). This effect strongly depends on the distribution of the different particles in the sample.

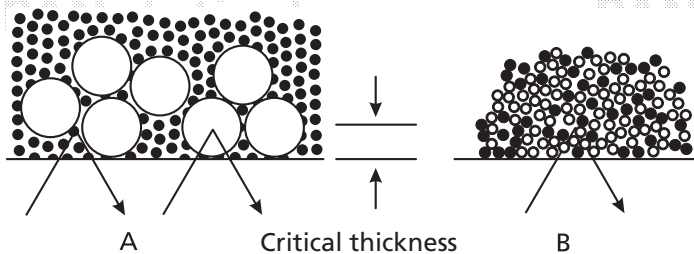


Figure 30. Effect of different particle sizes on resulting intensities (micro-absorption)

Figure 30 demonstrates the influence of both the differences in particle size and/or the absorption in a mixture of two phases:

- Part A shows
1. The effect of the crystallite size. The particles have different crystallite sizes.
 2. Micro-absorption. The particles differ in their absorption coefficients μ . In this figure the white circles represent particles with a higher absorption. Absorption contrasts (the ratio between the two μ 's) larger than about 5 means that the intensity ratios will be significantly wrong and therefore the quantification will be incorrect

Part B of the figure shows the ideal powder mixture.

The effect on the intensity is the same for both examples. The beam either passes the black particles and stops in a white particle, or it stops in a white particle without having 'seen' any black particles. So the white particles form the 'preferred phase', delivering a higher granularity quantity.

Extinction

Extinction is another effect that decreases intensity. The kinematic theory is not applicable as the crystallites have a too high degree of perfection. A reduction of intensity is due to an interference effect from secondary reflections of the diffracted beam from the undersides of the atomic planes, destructively interfering with the incident beam (phase shift 180° is given).

7.2.3 Limit of detection, limit of quantification, amorphous amounts and crystallinity

Limit of detection

Following the rules of the statistics of a Poisson distribution, the absolute and relative standard deviations σ and σ_{rel} of a measured number of counts N at a 2θ position are given by:

$$\sigma = \sqrt{N}$$

$$\sigma_{\text{rel}} = \frac{\sqrt{N}}{N} = \frac{1}{\sqrt{N}}$$

A usual criterion for the limit of detection (LOD) of a particular reflection, is that $N_{\text{reflection}} > N_{\text{background}} + 3\sigma_{\text{background}}$

Example: Measuring an N_{max} of 10,000 counts, the σ_{rel} is 0.01, corresponding to a relative error of 1%, the counting statistical error.

Note: Imagine we have a background of 100 counts and a small hump of 120 counts. Clearly this cannot be classified as a reflection because $3\sigma_{\text{background}} = 30$ is obviously higher than 20. The only solution is to increase the measurement time to improve the peak-background ratio.

Limit of quantification

On the other hand, the limit of quantification (LOQ) depends on the sum of the possible influences on the intensity: particle size, preferred orientation, line overlap, crystal symmetry, matrix effects, and amorphous amount. So in many cases the LOQ of a phase must be carefully determined by a calibration curve.

Amorphous amounts in mixtures

An automated determination of amorphous amounts can be carried out

- using a full-pattern fitting method (for example Rietveld method) of a measurement with a simulated amorphous content
- adding an internal standard and evaluating both measurements before and after the addition with a full-pattern fitting method.

Percentage crystallinity determination

The percentage of crystallinity (%C) of a sample is defined by the ratio of the total intensities in the diffraction peaks I_{net} and of the sum of *all* measured intensities I_{tot} , including the amorphous part and air scatter. The total air scatter intensity I_{scat} must be determined separately (by measuring a zero-background holder) and then subtracted, yielding

$$\%C = 100 \cdot \frac{\sum I_{\text{net}}}{\sum I_{\text{tot}} - \sum I_{\text{scat}}}$$

If the pure amorphous phase is available, the ratio C between the crystalline and the amorphous part of a material can be determined by using diffraction patterns at each 2θ position of the pure amorphous (a) and the pure crystalline (c) sample in combination with the mixture:

$$I(2\theta) = m(c I_c(2\theta) + (1-C) I_a(2\theta))$$

$I(2\theta)$ intensity at positions 2θ of the actual sample and of both the pure amorphous (a) and the pure crystalline (c) sample

m sample mass

The three diffractograms have to be corrected for air scattering by measuring a reference sample. This formula is, strictly speaking, only valid for an amorphous compound with the same elemental composition and the same density as the (mean value of the) crystalline compound(s).

All measurements have to be carried out using the same instrument settings and the same scan range parameters.

7.3 Methods of quantitative phase analysis

There are several possibilities to classify the different methods of quantitative phase analysis (for more information refer to KLUG & ALEXANDER and JENKINS & SNYDER).

Selecting the optimum method, depends on the answers to several questions:

- Which type of materials is being investigated: bulk material or powder?
- Do we need a complete phase analysis of all phases or only of one phase?
- Which standard material are available? Especially standard(s) for the required phase or phases?
- Will there be problems regarding absorption effects by adding a standard?
- What about possible overlaps of the reflections of the standard?
- Are all phases and their crystallography known in case we want to use the Rietveld method?
- Is a semi-quantitative analysis sufficient, for example the RIR (reference intensity ratio) method?
- Is it a recurring application requiring the use of a calibration curve?
- Which methods are supported by the software available to you?

A decision tree for the possible methods is given in Figure 31.

Starting with the basic question, whether a single or multi-phase quantitative phase analysis is required, the different methods are given regardless of existing conditions, like structure data, RIR values, standards or additional problems, for example the determination of the amorphous amount.

Finally, every problem can be solved - either as a routine method or by being strenuous in time and measurements leading to (semi)quantitative results.

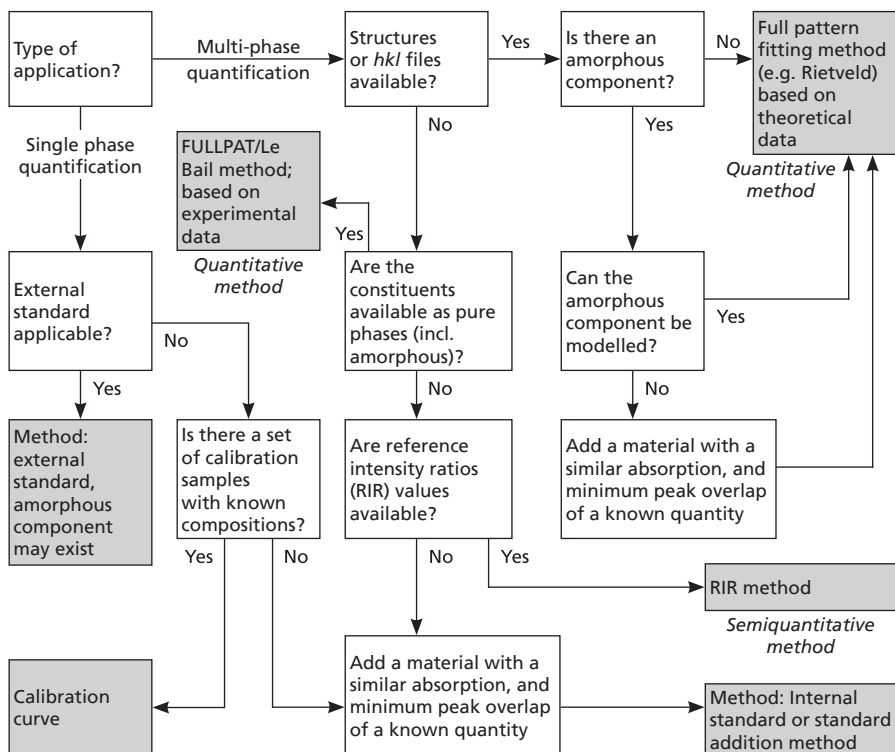


Figure 31. Decision tree for quantitative analysis

There are some aspects which should be considered when selecting a standard material:

It should:

- be available over a long period of time to enable investigations to be compared with each other.
- be possibly an internationally recognized standard material.
- be chemically stable (no oxidation or hydration).
- be mechanically stable.
- have a sufficiently small crystallite size.
- produce reflections with high intensities, because the quantitative results also depend on the counting statistics.
- not have fluorescent radiation.
- show as few peak overlaps as possible.
- be a substance with an absorption coefficient similar to that of the mixture to prevent micro-absorption effects.

Absolute calibration methods directly relate the measured intensities to the concentrations of the corresponding phase(s), measured for example as pure standard(s) or given as theoretically determined intensities.

- Advantage: Fast and easily applicable
- Disadvantages: The substance which has to be determined (or another one) must be present as a standard.
An absorption correction is necessary.
All measurements must be performed under identical measuring conditions.

Note that the stability of the incident beam intensity has to be monitored. This is done by repeated measurements of the maximum intensity of a reflection of a standard sample. The intensity of the standard is used to calculate a correction factor for the intensity of the sample measurements at a given time.

Addition methods relate the intensity of the phase of interest in the original sample with the intensity of the sample after the addition of a known amount of the same phase.

- Advantages: The absorption correction can be neglected.
Instrumental (intensity) variations are eliminated by using internal intensity ratios.
- Disadvantages: It is complicated to use for multi-phase mixtures.
The phase of interest must be available as pure substance.

Relative calibration methods (matrix flushing, internal standard) divide the intensities of the analytical phases by the intensities of reference or standard phases as a calibration curve before relating them to the phase concentrations.

- Advantages: The intensity ratios compensate the instrument (intensity) variations.
Arbitrary standard materials are useable.
The absorption correction can be ignored.
The calibration curve can be examined for further evaluation.
- Disadvantage: It may be time-consuming to build up a calibration curve.

7.4 Examples

7.4.1 Discussion of different methods

Spiking method

Figure 32 shows an example diffractogram of a mixture of the two TiO_2 modifications rutile and anatase.

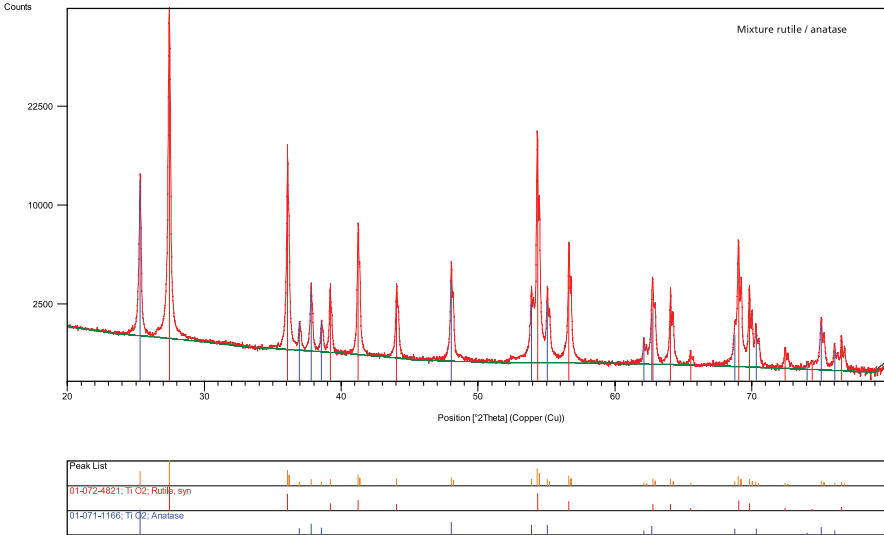


Figure 32. Typical diffractogram of a mixture of anatase and rutile, $\text{Cu K}\alpha$

For the intensity ratio of the sum of (all) integral intensities $I_{(hkl)A}$ and $I_{(hkl)R}$ the following applies:

$$\frac{I_{(hkl)R}}{I_{(hkl)A}} = \frac{R_{(hkl)R} \rho_A m_R}{R_{(hkl)A} \rho_B m_A}$$

Per gram of the mixture the quantity z_R of rutile is added. Then applies

$$\frac{I_{(hkl)R}}{I_{(hkl)A}} = \frac{R_{(hkl)R} \rho_A m_R + z_R}{R_{(hkl)A} \rho_B m_A} = S(m_R + z_R)$$

S is the slope in the representation $I_{(hkl)R} / I_{(hkl)A}$ as $f(z_R)$. The intersection of the straight line with the x axis delivers the amount m_R (note: $y = S_x + S z_R = 0$).

In the following example (Figure 33) for each 1 g of the original mixture pure rutile was added in amounts of 50 mg, 125 mg, 200 mg, 280 mg and 330 mg. (Note: sample is different from the one shown in Figure 32).

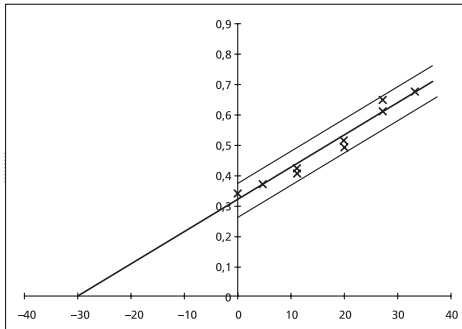


Figure 33. Spiking method for an example mixture, $m_{\text{rutil}} = 30.2 \pm 5.2 \text{ wt.}\%$ (confidence interval 95%)

Axes : y: Ratio of intensities of both phases
 x: left : - wt.% / right : Added gram per gram $\times 100$

Using the Rietveld method for the same sample, which is well established for this problem, the rutile content is determined to be $28.5 \pm 0.5 \text{ wt.}\%$.

Semi-quantitative methods are used if calibration standards and pure phases are not available - but the reference intensity ratios (RIR) or I/I_c - values are published. The I/I_c - values are given by the ICDD (for Cu radiation only) and correspond to a 50:50 mixture of the phase and corundum. Analysis is automatically performed when RIR values of the accepted candidates are available (see Figure 34, HighScore software).

Advantage: Easy to use
 Disadvantage: It might be necessary to determine your own I/I_c - values, sample texture and grain size effects give wrong results.

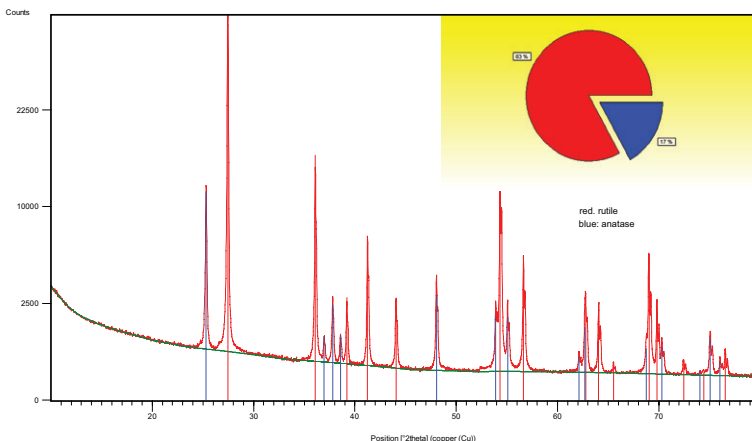


Figure 34. RIR analysis of example in Figure 32

Full pattern methods (especially the *Rietveld* method) compare the complete measured diffractogram with calculated diffractograms of all phases based on their crystal structure data.

The method is based on the minimization of the sum of the weighted squares of the deviations between the observed and the theoretical intensities of the diffractogram. The theoretical diffractogram is calculated from the crystallographic and structure data of the phases.

The Rietveld method was first introduced for structure refinement of neutron diffraction experiments (H.M. RIETVELD, 1969). It can also be used for structure refinement of X-ray data, but is preferably used as a standardless quantification method in many fields (cement, mineralogy and so on).

The main advantages of the Rietveld method are:

- Differences between the experimental standard and the unknown substance are minimized, which is important for the quantification of mineralogical samples with high variability.
- The demand for experimental data on pure standard samples is no longer necessary.
- Reflection overlaps do not influence the quantification result.
- The lattice parameters of the individual phases and the reflection profiles are refined.
- The accuracy of the quantitative phase analysis is improved, since the entire diffractogram and not just one or a few reflections are included in the evaluation.
- The influence of texture can be corrected, because it is included in the refinement.
- Absorption effects and the influence of the micro-absorption are modeled and considered.
- The determination of amorphous amounts is included.
- Crystallite sizes are calculated.
- The chemical composition is calculated. A comparison to the X-ray fluorescence analysis of the sample can confirm the reliability of both results.
- It works well when implemented into routine processes, for instance for production control in cement plants.
- Errors of quantification of less than 1 % are achievable.

The major disadvantage of the method is that the structure data of all phases in the sample have to be known. The currently available structure databases incorporate most of the common phases and can easily be extended by experimentally determined structure data, given for example as CIF or hkl files.

7.4.2 Determination of retained austenite

The determination of retained austenite in hardened steels is an important application of X-ray phase analysis. Austenite is a high-temperature phase in hardened steels. During cooling, most of the austenite transforms to the low-temperature phase martensite. However, a certain amount of the austenite is not converted, therefore being 'retained austenite'. Since this substantially affects the mechanical characteristics of the hardening structure, there is very much interest in its determination, especially because X-ray analysis is a reliable and non-destructive method.

The external standard method is not applicable because neither pure austenite nor pure martensite phases can be produced. Nevertheless, determining the retained austenite is an uncomplicated routine procedure. It is straightforward, because the R values for the reflections and different wavelengths are well known (see Chapter 7.1, FANINGER & HARTMANN) and $\mu_k' = \mu_k$ is valid (see Chapter 7.3):

$$R = \left(\frac{F_{hkl}}{V_{uc}} \right)^2 H P L$$

The accuracy of the result decreases with increasing concentrations of alloy elements. This requires a modification of the R values. Since as many reflections as possible should be used in the calculation, the use of Mo radiation is strongly recommended.

Note that additional international norms exist for this type of quantification.

7.4.3 Quantification of cement

Figure 35 shows a typical clinker diffractogram with more than 200 peaks in the 2θ range between 10° and 65° . Because of the multiple line overlaps and the large number of phases, only full-pattern methods are applicable for quantifying all phases. The phase composition allows the cement producer to optimize the production process parameters. As an example, the quantity of certain phases gives information on the hardening behavior and the compressive strength (for example alite amount) or the efficiency of the cement mill (sulfate phases).

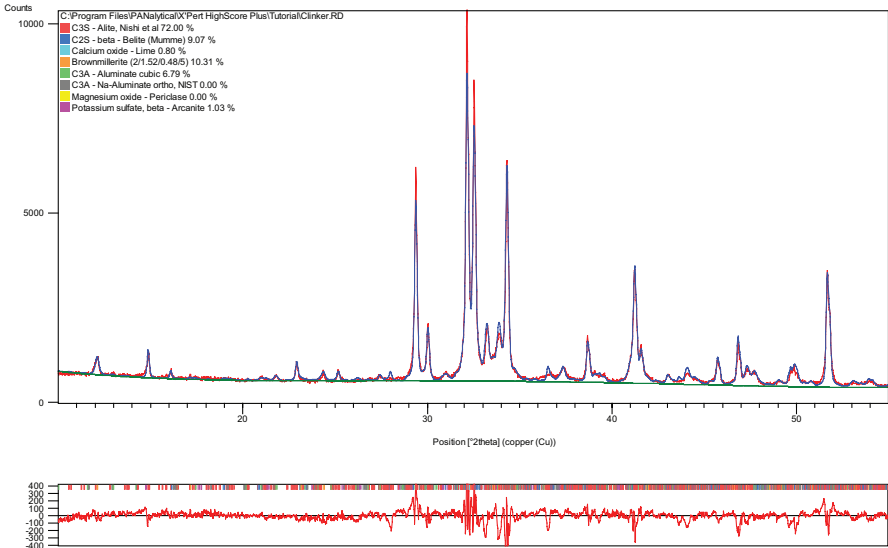


Figure 35. A clinker diffractogram showing the experimental pattern as well as the result of the Rietveld refinement, together with the difference plot

PANalytical

PANalytical

PANalytical

8. Crystallographic analysis

This type of analysis is usually carried out on single phase samples. The aim is to gain a better understanding of the crystallographic structure, ranging from unit cell refinement to structure solution.

8.1 Indexing

In the indexing or unit cell search procedure, hkl values are assigned to the reflections in the powder diffractogram. There are several routines described in the literature, for example:

DICVOL (04)
ITO
TREOR
McMaille

Based on at least 20 to 30 reflections, the various programs propose the various possible unit cells. The main criteria for a good solution are:

- a complete indexing of all reflections, if possible
- a high FOM (figure of merit),
- the lowest volume of the unit cell and/or,
- the agreement with the known density including the number of atoms/ molecules per unit cell.

Once possible unit cells have been found, the next step is to refine a selected unit cell and to decide on a lattice and possible space group by recalculating the pattern and looking for systematic extinctions.

Indexing can be very helpful to determine whether a sample consists of one phase or more (for example: to detect crystalline impurities).

Generally, to obtain a correct indexing of the diffraction pattern, it is necessary to use high-quality powder diffraction data that is free of experimental errors such as sample displacement or a zero shift.

8.1.1 Lattice parameter determination and refinement

When the unit cell (meaning the lattice parameters) is known, either from a qualitative phase identification or from an indexing, it is possible to refine the lattice parameters. That may be important for example for atomic substitution studies or optimization of certain processing parameters.

Often, a lattice parameter refinement is carried out as part of a full pattern quantitative analysis method, for example the Rietveld method.

8.1.2 Structure refinement

When the crystallographic structure of the material is known, it is possible to refine the complete set of structure parameters, like the atomic positions, occupation factors, atomic replacements, temperature factors and so on. This is the classical use of the Rietveld method: matching the total experimental pattern by refining both instrumental and structure parameters until the best fit is reached.

8.1.3 Structure solution

In general, it is very difficult to determine the structure of an unknown material from powder diffraction data. Single crystal X-ray diffraction is the preferred technique for this type of work. However, in certain cases it is not possible to obtain a large perfect single crystal suitable for single crystal diffraction analysis. In those cases one can try to propose a structure using high-quality powder diffraction data. For a successful structure solution, the expected crystal structure should be known.

9. Microstructural analysis

9.1 Residual stress

9.1.1 Basics

Residual stress is mechanical stress, which is present in a material independently of outside forces and/or moments. X-ray diffraction is an important method to determine the residual stress by analyzing the interplanar spacings $d(hkl)$ in different directions.

If a material has a tensile state (or a material is stressed by an axial tensile state), then the distances of the interplanar spacings, which are perpendicular to the tension, are increased, while lattice planes parallel to the tension experience a compression (due to the Poisson contraction).

Residual stresses change the interplanar distances and thus the diffraction angles 2θ (derivation of Bragg's law). By measuring the change of the diffraction angle ($\Delta 2\theta$) the lattice extension ε can be determined:

$$\varepsilon = \frac{d - d_0}{d_0}$$

Figure 36 shows the definition of the angles used in stress analysis.

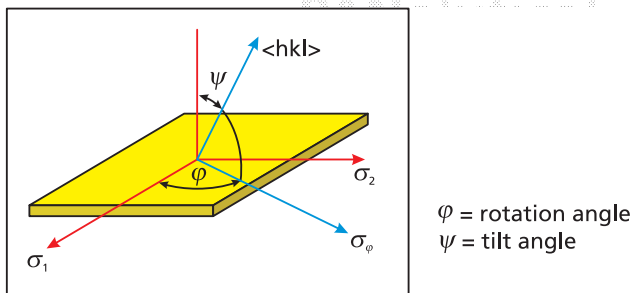


Figure 36. Definition of angles in stress analysis

Now, if the coordinate system is put in such a way into the surface that the ε_3 direction is the direction of the surface normal, then the extension $\varepsilon_{\varphi,\psi}$ of the sample surface follows from the main equations of the elasticity theory for the two axial tensile state delivering the basic equation of the X-ray residual stress determination:

$$\varepsilon_{\varphi,\psi} = \frac{d_{\varphi,\psi} - d_0}{d_0} = s_1^{r\ddot{o}} \sigma_1 + \sigma_2 + \frac{1}{2} s_2^{r\ddot{o}} \sigma_\varphi \sin^2 \psi$$

$d_{\phi,\psi}$	strained d -spacing with tilt angle ψ and rotation angle ϕ
d_0	strain-free d -spacing
σ_1, σ_2	stress of the normal of the diffracting lattice plane, see Figure 36
$s_1^{ro}, \frac{1}{2} s_2^{ro}$	X-ray elastic constants (XEC's)
$\varepsilon_{\phi,\psi}$	lattice extensions in the directions ϕ and ψ
ϕ	rotation angle
ψ	tilt angle

X-ray measurements are always carried out along the normal of the diffracting lattice plane (hkl). Due to the small penetration depth of the X-rays σ_3 can be set to 0 and it follows

$$\sigma_{\phi} = \sigma_1 \cos^2 \phi + \sigma_2 \sin^2 \phi$$

The indicated X-ray elastic constants s_1 and $\frac{1}{2} s_2$ of σ_1 and σ_2 are connected by the Voigt abbreviations with the material parameters ν and E (valid for isotropic materials):

$$s_1 = \frac{-\nu}{E} \quad \frac{1}{2} s_2 = \frac{\nu+1}{E}$$

E Young's modulus (modulus of elasticity)
 ν Poisson ratio (transverse contraction ratio)

9.1.2 $\sin^2 \psi$ method

By determining the slope m in the graph $d_{\phi,\psi} = f(\sin^2 \psi)$ or $\theta = f(\sin^2 \psi)$ the stress σ_{ϕ} can be determined:

$$\frac{m}{d_0} = \frac{1}{2} s_2 \sigma_{\phi} = \frac{1}{d_0} \frac{\Delta d_{\phi,\psi}}{d \sin^2 \psi}$$

Figure 37 shows an example of a $\sin^2 \psi$ plot, exhibiting slight compressive stress.

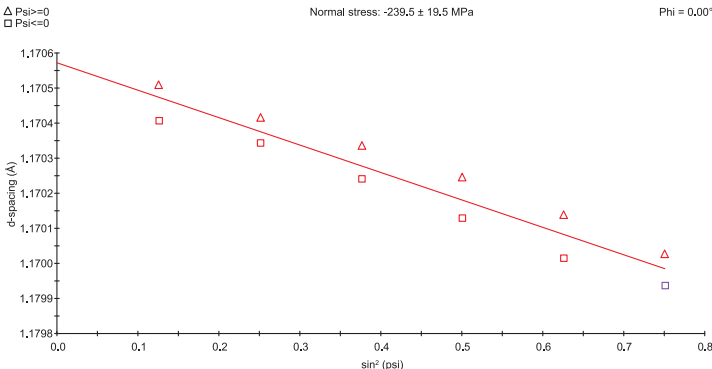


Figure 37. $\sin^2 \psi$ plot of a steel sample, using the (211) reflection

The $\Delta 2\theta$ increases with larger diffraction angles 2θ . Therefore reflections with higher angles are preferred for residual stress analysis. This might require longer X-ray wavelengths like Cr or Co radiation. However, when changing to longer wavelength, the information depth will be decreased. Also, different line overlaps can occur.

The irradiated area of the sample should be as small as possible, since during sample tilting the absorption depth in the sample changes. Hence the tube point focus should be used together with point focus collimators or X-ray lenses.

The different methods of determining the reflection maxima/ d spacings (e.g. cross correlation method, center of gravity, parabola etc.) are available in special analysis software like PANalytical's Stress software. All methods have their advantages and disadvantages, so you should choose the one that meets your requirements best.

9.2 Texture

9.2.1 Basics

In a crystal, atoms form a three-dimensional periodic arrangement (crystal lattice). This periodicity is constant within a crystallite and ends at the grain boundaries.

Polycrystalline materials consist of crystallites varying in shape and size. In practice the orientations of the crystallites are not randomly distributed like in an ideal powder specimen. Preferred orientations occur, which are called texture. These preferred orientations are connected to an interplanar spacing $d(hkl)$.

Texture can be caused by the production process or during treatments (for example: plastic deformation of bulk materials like rolling, pultrusion and so on), by crystal growth (epitaxy, rapid solidification) or during the preparation of powders.

Since the results of the qualitative and quantitative phase analyses are substantially affected by textures, this has to be taken into consideration or needs to be minimised as much as possible, see Chapter 7.2.

Note that textures are not necessarily disadvantageous for the property of materials. They are highly desired in some cases, for example in electrical, magnetic or also mechanical components, since the anisotropy is the basis for certain physical properties such as superconductivity. In these cases texture analysis is used to characterize and quantify the structure / property relation.

Measurement

A texture measurement is performed by rotating the sample around the surface normal ($\Delta\varphi$) and tilting it perpendicular to the beam direction ($\Delta\chi$) while setting the goniometer to a fixed 2θ - position corresponding to the selected lattice plane/ reflection (i.e. d value). A point detector is used together with a large receiving slit. A line detector in receiving slit (OD) mode can be used as well.

Pole figure

The result of a texture analysis is displayed as the so-called pole figure, which is a two-dimensional graphical representation (e.g. stereographic projection) of the intensity distribution of a particular Bragg reflection relative to the sample surface, see Figure 38.

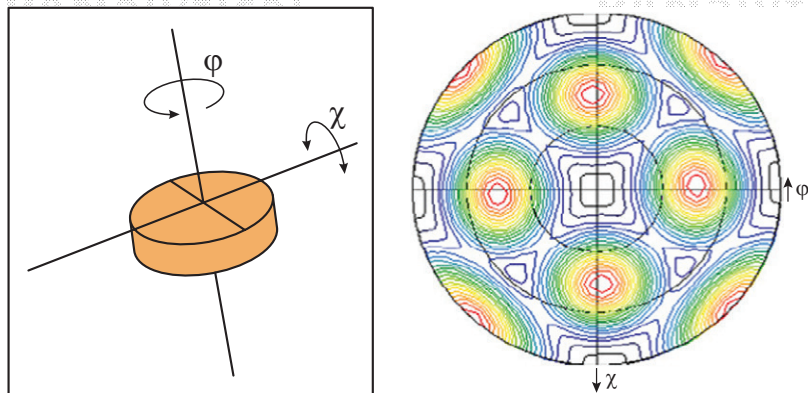


Figure 38. Representation of the intensities of a certain set of $\{hkl\}$ planes with respect to the sample reference frame (pole figure)

Orientation distribution function

The orientation distribution function (ODF) can be determined from a set of independent pole figures and gives a quantification of the texture. The intensity of the ODF indicates the volume fraction of the crystallites with a certain orientation.

9.2.2 The Lotgering factor

The Lotgering factor (F) represents a simple but nevertheless very useful way to give a statement on the quantitative amount of texture of a certain orientation.

It is defined by the equation

$$F = \frac{P - P_0}{1 - P_0}$$

For example for a (001) texture, the value P is the sum of the integral intensities of all (001) directions divided by the sum of all intensity (hkl) directions in the textured sample. P_0 is the equivalent factor for the irregularly oriented sample.

$$P = \frac{\sum I_{001}}{\sum I_{hkl}}$$

The factor F varies between 0 for a completely random orientation in the sample and 1 for a completely oriented sample.

9.2.3 Omega scan

Another simple method to quantify a texture is to perform an Omega scan. When varying Omega at a fixed 2θ , a randomly oriented sample produces a constant intensity. On a sample with a preferred orientation a peak will be observed, representing the preferred orientation of the lattice planes in one direction. The full width at half maximum (FWHM) of the peak describes the amount of a texture. For precise analysis a texture-free sample should be measured first to correct for beam path influences which lead to intensity changes while tilting (e.g. defocusing effects).

9.3 Crystallite size determination

9.3.1 Basics

The full width at half maximum of a reflection depends both on the diffractometer geometry and the setup (slits, optics, 2θ angle, detector, etc.) and on the sample itself. Under ideal conditions (for example: smallest divergence of the monochromatic beam and a 'perfect' sample with crystallite sizes between 0.5 and 5 μm without crystal imperfections) a standard powder diffractometer can produce diffractograms with peak widths (FWHM) between 0.03° and 0.1° 2θ over the whole angular range.

Peak broadening caused by the sample can be explained by the presence of very small crystallites and/or micro-strain.

9.3.2 Crystallite size

The well-established Scherrer equation describes the relation between the broadening of the reflection and the average crystallite size τ :

$$\tau = \frac{K\lambda}{\beta_{\tau} \cos \theta}$$

β_{τ}	Broadening of the reflection due to small crystallite sizes with $\beta_{\tau} = (B - b)$	B FWHM of the reflection of the real sample b FWHM of the standard reflection (crystallite size approx. 0.5 to 5 μm) Note that β_{τ} is indicated in rad!
K	approx. 0.9 (0.89 for spherical, 0.94 for cubic crystallites)	
λ	wavelength	
θ	diffraction angle	

Figure 39 describes the line broadening effect given by decreasing crystallite sizes. Its influence will be stronger than instrumental broadening for crystallite sizes much smaller than 1 μm .

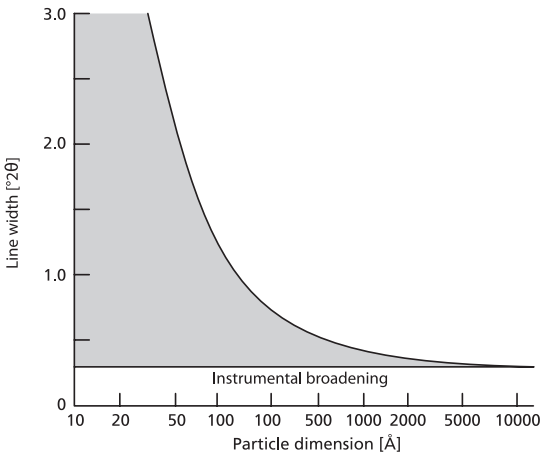


Figure 39. Line broadening as a function of the crystallite size, in addition to instrumental broadening (from JENKINS, SNYDER, 1996)

9.3.3 Micro-strain

The peak broadening β_{ε} is related to micro-strains ε , for example those caused by defects or atom substitution, as given in the Wilson equation:

$$\varepsilon = \frac{\beta_{\varepsilon}}{4 \tan \theta}$$

β_{ε} Broadening of the reflection due to lattice strain
 with $\beta_{\varepsilon} = (B^2 - b^2)^{1/2}$ B FWHM of the reflection of the real sample
 b FWHM of the standard reflection
 (crystallite size approx. 0.5 to 5 μm)
 Note that β_{τ} is indicated in rad!

θ diffraction angle

9.3.4 The Williamson-Hall plot

To distinguish between broadening by strain and broadening by crystallite size the reflection profile can be analyzed. The peak profile should be symmetrical. Asymmetric profiles are due to effects caused by the Soller slit opening (axial divergence) or depth gradients of the sample. The broadening by crystallite size leads to a Lorentz profile, the broadening by micro-strains leads to a Gaussian profile.

Since crystallite- and/or micro-strain-induced broadening differ in their angular dependence ($1/\cos\theta$ and $\tan\theta$ respectively) both effects can be separated.

This is done by the Williamson-Hall plot as presented in Figure 40. It can be easily derived from the fitted peaks of a full diffraction pattern (functionality of HighScore Plus package). The example shows a particle size of about 61 nm and a slight micro-strain of 0.15%.

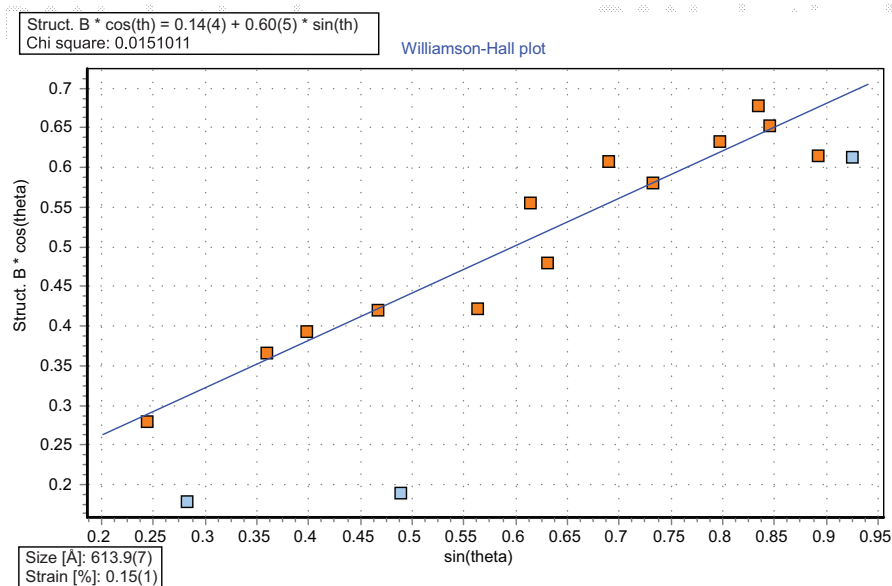


Figure 40. Example of Williamson-Hall plot (blue: excluded peaks)

9.3.5 Discussion of the peak broadening

The following figures explain the possible influences on line broadening, now including the residual stress (see Chapter 9.1) and the influence of the thermal treatment of the material.

Figure 41 distinguishes between the different influences of strain on the position and the broadening of the reflections.

Figure 42 demonstrates the healing process of a rolled material depending on the temperature. There is no movement of the reflection position.

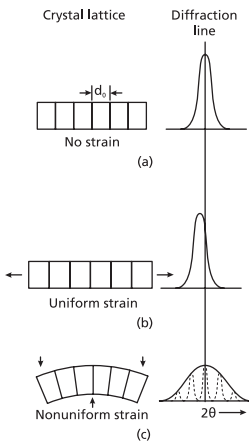


Figure 41. Influence of strains both on position and FWHM of the reflections

- a) unstrained
- b) uniform strain
- c) non uniform strain

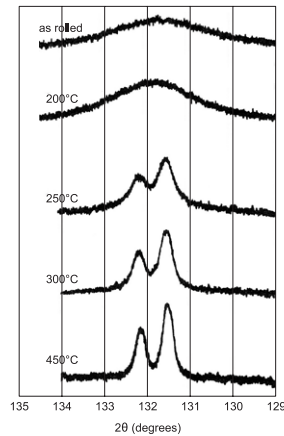


Figure 42. Influence of thermal treatment on the healing process

(from JENKINS, SNYDER, 1996)

10. Non-ambient XRD

A further application of X-ray powder diffraction is the investigation of the behavior of materials under non-ambient conditions, for example higher/lower temperatures, controlled humidity, high/low pressures, vacuum, inert or reactive gas atmospheres, stress, electromagnetic fields, etc.

The investigation of non-ambient processes imposes special demands on the instrument and the software. The emphasis is on the investigation of phase transitions and the measurement of the stability of existing phases. Also, the expansion or contraction of the lattice under non-ambient conditions can be studied.

Modern powder diffractometers with dedicated non-ambient chambers allow a quick and precise exchange between normal and non-ambient experiment setups and offer computer control and logging of the non-ambient variables.

10.1 Temperature

The most-widely used non-ambient variable is temperature. Low- and high-temperature chambers are available for both reflection geometries and capillaries for transmission. The possible temperatures range from 4 K up to more than 2000 K, using different types of non-ambient chambers. The chambers can be built as a reactor for high pressures, for aggressive gas mixtures or for investigations under computer-controlled humidity.

The commercially available non-ambient chambers can be divided in two types:

- Direct heaters/coolers, where the sample is attached directly to a heating strip or cooling block (see Figure 43, left).
- Indirect heaters, where the sample is heated by a surrounding oven (see Figure 43, right).



Figure 43. Anton Paar TTK 450



Anton Paar HTK 1200N

There are three additional issues to be taken into account when performing non-ambient experiments:

- Correct adjustment and possible changes in position of the sample, causing shifts of the reflections
- Additional requirements for sample preparation, especially for high temperatures
- Determination of the actual sample temperature

10.1.1 Correct sample positioning and height

The accurate height of the sample is critical for accurate measurements. A stable sample height at non-ambient temperatures is thus very important, especially in reflection geometry. There are various solutions to this problem, depending on the type of non-ambient chamber:

- Correction of height error in the software by
 - using a pre-determined expansion calibration of the empty sample holder
 - addition of an internal standard
- Active correction of sample height with a computer-controlled height adjustment stage, for example by using a pre-calibrated function
- Use of parallel beam geometry, e.g. a parabolic X-ray mirror and a parallel plate collimator

The right choice is especially important when working at low angles of incidence, for example when investigating thin films.

The problem can be ignored if only phase transitions shall be observed.

10.1.2 Sample and preparation

Capillary geometry

If the sample is in powder form, the capillary geometry is the best technique to minimize texture effects. Because of indirect heating the maximum temperature is limited to about 900°C, using quartz capillaries. For low temperature measurements there are special devices available. They provide a cold laminar gas stream surrounding the capillary.

The sample amount and the reaction volume can be minimized in the capillary geometry. By sealing the capillary, a controlled environment can be achieved, so that for example oxygen or humidity from the ambient air cannot influence the experiment.

The use of capillaries is also advantageous for samples that react with metallic heating strips. Since only indirect heating is available, the maximum temperature is limited.

Reflection geometry

Bulk materials or powders are put on a heating strip or a special sample cup.

The direct or indirect heating has to assure a uniform heating with a minimal temperature gradient. Small sample amounts (and samples with high thermal

conductivity) are favored. In this setup, very high temperatures above 2000°C are possible.

The arrangement in reflection geometry is favorable for solid samples, investigations of layers, samples in reactors, and 'open' systems. The reflection geometry is also advantageous for substances that react with quartz or glass capillaries.

Possible reactions between the sample and the sample carriers (e.g. glass, Pt, Ta, W, steel, corundum) and/or the inert gasses or an oxidative atmosphere have to be considered. Also, the emission of reactive gasses during the temperature treatment could damage the interior of the temperature chamber.

10.1.3 Temperature measurement and calibration

The temperature measurement is generally done by thermocouples. For higher temperatures (> 1200°C) pyrometers can be used additionally.

The thermocouple has to be as close as possible to the sample in order to minimize temperature differences. This is especially problematic when using strip heaters, where the thermocouple is mounted at the bottom of the strip. In addition, the contact between the strip and the sample is an issue, as well as the temperature gradient between the bottom and the top of the sample and towards the sides.

Table 10 provides a list of candidates for a high-temperature calibration, showing both phase transitions and melting points, up to 2000° C. Make sure that the calibration is done under exactly the same conditions as the actual experiment (location of the temperature measurement, gas flow or vacuum etc.). The expansion coefficients for BN and MgO are also given and might be helpful.

10.1.4 Special requirements

There are some further requirements to the experiment, regarding

- the chamber windows (foils):
 - these are often smaller than the size of the line focus
 - they produce additional absorption or even scatter, which can appear as a broad reflection at low angles
- the atmosphere inside the chamber:
 - different absorption behavior of the X-rays
 - influence on the temperature measurement
- a fast detector with a simultaneous registration to ensure short measuring times in order to allow real-time *in situ* observation of the processes
- the software packages, which have to control the temperature for temperature profiles with heating rates, waiting times and scans, saving them together with the actual temperatures and allow reporting of the actual temperature profile. Display of phase transitions in the analysis software package can be done for example as isolines diagram (see example in Figure 44)

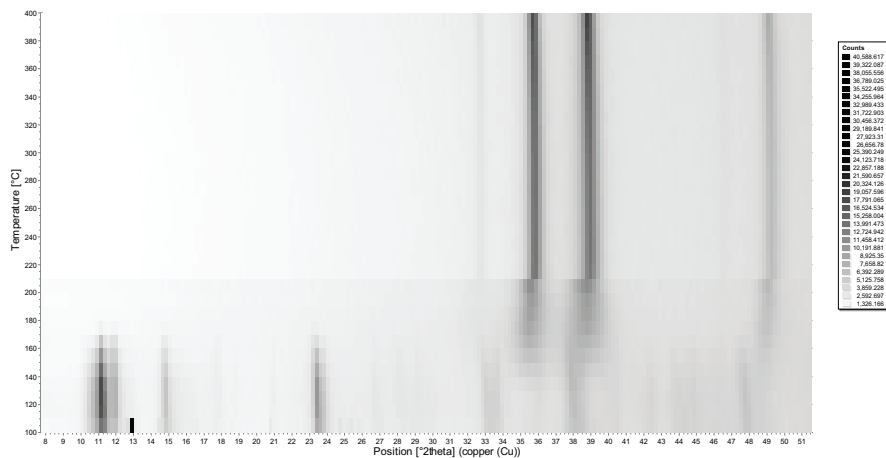


Figure 44. Example of a non-ambient (temperature) phase transition experiment



Table 10. Some temperatures for calibration using phase transitions / melting points

substance	phase transition	melting point temperature / (°C)	
NH ₄ NO ₃	orth. ==> tetr.; moist		84.2
	tetr. ==> cubic; moist, dry		125.2
TiNO ₃	orth. ==> trig.		79
	trig. ==> cubic		143
KNO ₃	orth. ==> trig.		128
CsNO ₃	trig. ==> cubic		160
RbNO ₃	trig. ==> cubic		164
	cubic ==> tetr.		219
	tetr. ==> cubic		291
AgNO ₃	orth. ==> trig.		165
		Sn	231.9
KClO ₄	orth. ==> cubic		295.7
		Pb	327.5
		KNO ₃	333.6
		Zn	419.6
Ag ₂ SO ₄	orth. ==> hex.		427
		CuCl	430.0
Quartz	trig. ==> hex. (α ==> β)		573.0
		Sb	630.5
		Al	660.2
		KCl	776
		NaCl	804 ± 3
		Bi ₂ O ₃	820
		Ag	962.0
		NaF	988.0
		Au	1064.4
		K ₂ SO ₄	1069
		Cu	1083.0
		CaF ₂	1360
		Ca ₂ SiO ₄	α ==> α'
Ni	1453		
Co	1495		
Fe	1535		
Ti	1675		
Zr	1852		
Cr	1890		
Rh	1966		

Use of expansion coefficients:

BN: for $T = 20 \dots 900^\circ\text{C}$: $c / \text{\AA} = 6.6516 \text{\AA} + 2.74 \cdot 10^{-4} \cdot T$ MgO: $a / \text{\AA} = 4.2100 \text{\AA} \cdot (1 + 11.39 \cdot 10^{-6} T + 2.46 \cdot 10^{-9} T^2)$
(Taylor; Br. Ceram. Trans. J. 83, 1984)

10.2 Pressure

The operation of high-pressure devices requires a lot of safety precautions.

There are two basic types of high pressure chambers: conventional, commercially available high-temperature reactor chambers that allow the investigation of powders or solid materials under certain atmospheres and medium pressure of up to about 10 MPa (e.g. Anton Paar XRK 900), and special non-commercial high-pressure cells like diamond anvil cells.

The pressure cell is fully closed; it can either be used as a self-pressurizing system or can be pressurized by using a gas tube or compressor.

The diamond anvil cell consists of two diamond anvils with a metal foil between them. A hole (approx. 0.1 mm) in the metal foil takes the sample which is embedded in a liquid. The high hydrostatic pressure results from pressing the diamond anvils together, whereby the metal foil becomes smaller by plastic deformation, and thereby the hole, too. Static pressures up to 100 GPa are reachable.

In a different type of anvil cell (up to 10 GPa) from ALLAN, MILETICH & ANGEL the force is generated by four screws which, when tightened, draw two halves of the cell together. This force is then transmitted through the steel body of the cell, through the beryllium plates to the diamond anvils. The two anvils are brilliant-cut diamonds, almost the same as found in wedding rings except that small flat surfaces are ground on their tips. High pressure is generated because the area of the diamond tips or culets is much smaller than the area of the screw threads.

10.3 Humidity

Humidity chambers (e.g. Anton Paar CHC) allow the investigation of phase transitions and stabilities under a controlled humidity. It is normally combined with a heating and cooling facility to extend the applications to low- and high-temperature work. The relative humidity range from 5% to 95% is computer-controlled. The setup is ideal for investigating humidity and/or temperature-dependent structural changes of pharmaceuticals, fine chemicals, clays or zeolites.

11. Recommended literature

D.R. Allan, R. Miletich, R.J. Angel, *Rev. Sci. Instrum.* (1996), 67, 840

M.E. Bowden and M.J. Ryan, Comparison of Intensities from Fixed and Variable Divergence X-Ray Diffraction Experiments, *Powder. Diffr.* (1991), 6, 78

G.W. Brindley, The effects of grain and particle size on X-ray reflections from mixed powders and alloys, considered in relation to the quantitative determination of crystalline substances by X-ray methods, *Phil. Mag.* (1945), 36, 347 - 369

G. Caglioti, A. Paoletti & F.P. Ricci, Choice of collimators for a crystal spectrometer for neutron diffraction, *Nucl. Inst.* (1958), 3, 223 - 228

S.J. Chipera & D.L. Bish, Fullpatt: a full-pattern quantitative analysis program for X-ray powder diffraction using measured and calculated patterns, *J. Appl. Cryst.* (2002), 35, 744 - 749

F.H. Chung, Quantitative interpretation of X-ray diffraction patterns, I. Matrix-flushing method of quantitative multicomponent analysis, *J. Appl. Cryst* (1974a), 7, 513 - 519

F.H. Chung, Quantitative interpretation of X-ray diffraction patterns, II. Adiabatic principle of X-ray diffraction analysis of mixtures, *J. Appl. Cryst* (1974b), 7, 526 - 531

F.H. Chung, Quantitative interpretation of X-ray diffraction patterns, III. Simultaneous determination of a set of reference intensities, *J. Appl. Cryst* (1975)

W.A. Dollase, Correction of intensities for preferred orientation in powder diffractometry: Application of the March model, *J. Appl. Cryst.* (1986), 19, 267 - 272

G. Faninger, U. Hartmann, *Harterei Technische Mitteilungen* (1972), 27, 233-244

L.W. Finger, D.E. Cox & A.P. Jephcoat, A correction for powder diffraction peak asymmetry due to axial divergence, *J. Appl. Cryst.* (1994), 27, 892 - 900

X.F. Fischer, Divergence slit corrections for Bragg-Brentano diffractometers with rectangular sample surface, *Powder. Diffr.* (1996), 11, 17 - 21

J.D. Hanawalt, see: Appendix in: 'Search Manuals for the Powder Diffraction File', International Centre for Diffraction Data, Swarthmore PA, USA, (1988)

H. Herman & M. Ermrich, Microabsorption of X-ray intensity in randomly packed powder specimens, *Acta Cryst.* (1987), A43, 401 - 405

R.J. Hill and C.J. Howard, Quantitative Phase Analysis from Powder Diffraction Data using the Rietveld Method, *J. Appl. Cryst.* (1987), 20, 467

International Tables for Crystallography, Vol. A, Mathematical, Physical and Chemical Tables, ed.: A.J.C. Wilson, Kluwer, London (1995), (corrected reprint)

- R. Jenkins and R.L. Snyder, Introduction to X-Ray Powder Diffractometry, Wiley 1996
- T.H. de Keijser, J.L. Langford, E.J. Mittemeijer and A.B.P. Vogels, Use of the Voigt function in a single line method for the analysis of X-ray diffraction line broadening, *J. Appl. Cryst.* (1982), 15, 308-314
- L.A. Kelley, S.P. Gardner and M.J. Sutcliffe, An automated approach for clustering an ensemble of NMR-derived protein structures into conformationally-related subfamilies, *Protein Engineering* (1996), 9 1063-1065
- H.P. Klug and L.E. Alexander, X-ray Diffraction Procedures, Wiley, New York (1974), 661 pages
- J.L. Langford and A.J.C. Wilson, Scherrer after Sixty Years: A Survey and Some New Results in the Determination of Crystallite Size, *J. Appl. Cryst.* (1978), 11, 102-113.
- G.S. Pawley, Unit-cell refinement from powder diffraction scans, *J. Appl. Cryst.* (1981), 14, 357-361
- W.A. Rachinger, A correction for the $\alpha_1 : \alpha_2$ doublet in the measurement of widths of X-ray diffraction lines, *J. Sci. Instrum.*, 25, (1948), 254-259
- H.M. Rietveld, Line profiles of neutron powder-diffraction peaks for structure refinement, *Acta Cryst.* (1967), 22, 151-152
- H.M. Rietveld, *J. Appl. Cryst.* (1969), 2, 65-71
- M. Sato, Y. Sato and L.C. Jain, Fuzzy Clustering Models and Applications, *Studies in Fuzziness and Soft Computing* vol. 9, Springer group (1997), New York, 122 pages
- A. Savitsky and M.J.E. Golay, Smoothing & differentiation of data by simplified least squares procedures, *Anal. Chem.* (1964) 36, 8, 1627-1639
- P. Scherrer, Bestimmung der Grösse und der inneren Struktur von Kolloidteilchen mittels Röntgenstrahlen, *Nachr. Ges. Wiss. Göttingen*, (1918), 2, 96-100
- D.K. Smith, G.G. Jr. Johnson, A. Scheible, A.M. Wims, J.L. Johnson and G. Ullmann, Quantitative X-ray powder diffraction method using the full diffraction pattern, *Powder. Diffr.* (1987), 2, 73-77
- G.S. Smith and R.L. Snyder, a criterion for rating powder diffraction patterns and evaluating the reliability of powder indexing, *J. Appl. Cryst.* (1979), 12, 60-65
- R.L. Snyder, The Use of Reference Intensity Ratios in X-Ray Quantitative Analysis, *Powder. Diffr.* (1992), 7, 186-193
- Taylor; *Br. Ceram. Trans. J.* 83, 1984

J.W. Visser, A fully automatic program for finding the unit cell from powder data, J. App. Cryst (1969), 2, 89

P.E. Werner, L. Eriksson & M. Westdahl, TREOR, a semi-exhaustive trial-and-error powder indexing program for all symmetries., J. Appl. Cryst. (1985), 18, 367-370

D.B. Wiles and R.A. Young, A new computer program for Rietveld analysis of X-ray powder diffraction patterns, J. Appl. Cryst. (1981), 14, 149-151

E.R. Wölfel, Theorie und Praxis der Röntgenstrukturanalyse, Vieweg&Sohn 1989

P.M. de Wolff, A simplified criterion for the reliability of a powder diffraction pattern indexing, J. Appl. Cryst. (1986), 1, 108-113

R.A. Young (editor), The Rietveld Method, Oxford University Press, Oxford (1993), paperback (1995, 2000)



12. Symbols

The symbols used in formulas in this book are:

2θ	-	Angle between incident and reflected beam
α	-	Absorption coefficient
\AA	-	Ångström, a unit length of 10^{-10} m, or 0.1 nm
A	-	Amorphous sample
β_{τ}	-	Broadening of the reflection due to small crystallite sizes
C	-	Face centered unit cell
C	-	Crystalline sample
c	-	The velocity of light
%C	-	Percentage crystallinity
D	-	material
$d_{\varphi,\psi}$	-	Strained d -spacing with tilt angle ψ and rotation angle φ
d_o	-	Strain-free d -spacing
d	-	Interplanar spacing (better $d(hkl)$), $hkl\dots$ Miller indices
λ	-	The wavelength of X-rays
e	-	Elementary charge
E	-	Energy
E	-	Young's modulus (modulus of elasticity)
e^{-M}	-	Temperature factor
E_{kin}	-	Kinetic energy
$\varepsilon_{\varphi,\psi}$	-	Lattice extensions in the directions φ and ψ
F	-	All-face centered unit cell
f_j	-	Scattering factor of each atom j
H	-	Multiplicity factor
h	-	Planck's constant
ω	-	The incident beam angle
θ	theta	Bragg angle θ_b
I	-	Body centered unit cell
I	-	Transmitted intensity
I	-	Tube's emission current
$I(2\theta)$	-	Intensity at positions 2θ of the actual sample
$I_{(hkl)}$	-	Integral intensities
I_k	-	Scattered intensity of the individual phases
I_{scat}	-	Total air scatter intensity
I_{tot}	-	All measured intensities
I_o	-	Intensity of incident or primary beam
I_{wr}	-	Total intensity of the white radiation
K_o	-	Constant for the equipment
L	-	Lorentz factor
m_k	-	Mass portion
m_e	-	Mass of the electron
μ	mu	Attenuation coefficient
μ	mu	Attenuation
μ_k	-	Attenuation coefficient

N	-	measured number of counts
ν	nu	Frequency
ν	nu	Poisson ratio (transverse contraction ratio)
P	-	Polarization factor
P	-	Primitive unit cell
P_0		The equivalent factor for irregularly oriented sample
P		Packing fraction
ρ	rho	Density
ρ_k		Density of the phase k
φ	phi	Rotation angle
χ	chi	Tilt angle
Q_0		Cross-section of the incident beam
σ	sigma	Scatter
Σ	sigma	Absolute deviation
σ_{rel}		Relative standard deviations
σ_φ		Tension
τ		Absorption
τ		Average crystallite size
U		High-voltage difference
V_{uc}	-	Volume of the unit cell
v		percentages by volume of the individual phases
Z		Atomic number





1. Index

Symbols

0D detector – 38
1D detector – 38
2D detector – 38

A

Absorption – 60
Amorphous amounts – 62
Amorphous state – 18
Anatase – 66
Anode – 12
Area detectors – 42
ASTM – 56
Attenuation coefficient (μ) – 11

B

Bragg-Brentano – 30
Bragg-Brentano geometry – 33
Bragg's law – 22
Bravais lattices – 19
Bremsstrahlung – 13, 16

C

Calibration – 83
Capillary – 47, 49, 50
Capillary geometry – 82
Capillary measurements – 45
Cement – 69
Characteristic radiation – 16
Characteristic X-ray radiation – 13
Characteristic X-rays – 14
Clinker – 69
Cluster analysis – 56
Coherent or Rayleigh scatter – 11
Compton scatter – 11
Crystal classes – 20
Crystalline state – 18
Crystallinity – 28
Crystallite size – 28
Crystal structure – 17

D

Dauvillier law – 13
Debye-Scherrer 'cones' – 40
DICVOL – 71
Diffractogram – 27
d-I tables – 55
Duane-Hunt law – 13

E

Electromagnetic waves – 10
Epitaxy – 75
Ewald sphere – 21
Extinction – 61

F

Fluorescence – 11
Foil transmission – 47, 49
FOM (figure of merit) – 71
Full pattern methods – 68
Full width at half maximum – 36
FWHM – 36, 77

G

Gas proportional counter – 40
Gels, liquids – 46, 47

H

High-pressure devices – 86
Humidity chambers – 86

I

ICDD (International Centre for
Diffraction Data) – 56
Incoherent scatter – 11
Intensity I_0 – 11
Interplanar spacings – 20
ITO – 71

J

JCPDS – 56

K

K-edge – 15
K-shell – 14, 15
K β filter – 36

L

Lattice parameters – 71
Lattice planes – 20
L-edges – 15
Limit of detection – 62
Limit of quantification – 62
Line detectors – 41
LOD – 48
LOQ – 48
Low angles – 28
L-shell – 14, 15

M

McMaille – 71
Micro-absorption – 61
Micro-strains – 78
Miller indices – 20
Monochromator – 36
Monochromators – 37
Moseley law – 16

N

Non-ambient – 81

O

ODF – 76
Omega scan – 77
Orientation distribution function – 76

P

Particle size – 28
PCA (principal components analysis) – 57
PDF-2 – 56
PDF-4+ – 56
PDF-4/Minerals – 56
PDF-4/Organics – 56
PDF database
 (Powder Diffraction File) – 56
Peak profile – 78

Peak table – 55
Percentage crystallinity
 determination – 62
PIXcel^{3D} – 41
Point detectors – 40
Poisson ratio – 74
Pole figure – 76
Preferred orientation – 59
Pultrusion – 75

R

Rapid solidification – 75
Reciprocal lattice – 18
Reflection – 45
Reflection geometry – 30, 82
Reflection mode – 47, 48, 49, 50
Reflection profile – 78
Residual stress – 73
Resolution – 27
Retained austenite – 69
Rietveld method – 67, 68
Rolling – 75
Rough surfaces – 52
Rutile – 66

S

Scherrer equation – 77
Scintillation counter – 41
Search/match – 55
Semi-quantitative methods – 67
Soller slit – 78
Space groups – 20
Spiking method – 66
Synchrotrons – 12

T

Thin layers – 51
Transmission – 45
Transmission geometry – 32
Transmission mode – 50
TREOR – 71

U

Unit cell – 18, 71

V
Voigt abbreviations – 74

W
Wavelength – 10, 11
Wilson equation – 78

X
X'Celerator – 41
X-ray tube – 12

Y
Young's modulus – 74